Hydrofoiling Europe-Dinghy

Simon Karlsson and Jesper Urde

DIVISION OF PRODUCT DEVELOPMENT | DEPARTMENT OF DESIGN SCIENCES
FACULTY OF ENGINEERING LTH | LUND UNIVERSITY

2018

MASTER THESIS

Hydrofoiling Europe-Dinghy

Development of separate hydrofoils as complement to Europe-dinghies

Simon Karlsson and Jesper Urde

LUND UNIVERSITY

Hydrofoiling Europe-Dinghy

Development of separate hydrofoils as complement to Europe-dinghies

Published by

Department of Design Sciences
Faculty of Engineering LTH, Lund University
P.O. Box 118, SE-221 00 Lund, Sweden

Subject: Machine Design for Engineers (MMKM05)
Division: Department of Design Sciences
Supervisor: Johan Revstedt
Co-supervisor: Nils Bjerkås (Essiq AB)
Examiner: Axel Nordin

Abstract

The aim of this master thesis was to develop and build a prototype of separate hydrofoils compatible with a Europe-dinghy (A common, single sail, one-person dinghy), to be used as a proof of concept. This was to be done without causing any permanent changes to the dinghy's hull. The consulting firm Essiq AB supported the project.

Extensive benchmarking of existing foiling dinghies, already on the market, was carried out. Based on this, concepts of different configurations of a hydrofoiling Europe-dinghy were generated. After choosing the most promising concept, it was further refined. Simulations in computational fluid dynamics (CFD), and theoretical calculations were completed to optimize the final design.

A prototype of the final design was built and tested. The test proved positive, with successful foiling during shorter periods of time. Nevertheless, the prototype will need some further refinements in order to reach its full potential.

The conclusion drawn was that this was a successful proof of concept, and that attaching separate hydrofoils to a Europe-dinghy is therefore a viable option.

Keywords: Essiq AB, Europe-dinghy, Hydrofoiling, Product development, Sailing

Sammanfattning

Syftet med detta examensarbete var att utveckla och bygga en prototyp på separata bärplan till en E-jolle (en vanlig segeljolle avsedd för en person), för att kunna utföra en konceptvalidering. Detta skulle göras utan att permanent förändra E-jollens skrov. Konsultfirman Essiq AB stöttade projektet.

Utförlig riktmärkning genomfördes genom att studera bärplansförsedda jollar som redan existerade. Baserade på informationen som samlats in genererades koncept på olika konfigurationer av en bärplansförsedd E-jolle. När det mest lovande konceptet valts ut, utvecklades det vidare. Simuleringar i beräkningsströmningsdynamik (CFD) och teoretiska beräkningar genomfördes för att vidare optimera den slutgiltiga designen.

En prototyp av den slutliga designen byggdes och testades. Testet var framgångsrikt, då båten stundtals seglade uppe på bärplanen. Prototypen kräver dock en del förbättringar för att nå sin fulla potential.

Slutsatsen som drogs var att detta var en lyckad konceptvalidering och att användning av separata bärplan för en E-jolle därför är realiserbart.

Nyckelord: Bärplan, E-jolle, Essiq AB, Produktutveckling, Segling

Acknowledgments

This project could not have been completed were it not for the help and support received from knowledgeable and helpful individuals and companies. We would like to thank everyone that has been involved and made this project possible!

The following companies and institutions supported the project:

Essiq AB	This project has been carried out in close cooperation with Essiq AB. Apart from supporting the project financially, Essiq AB has provided help with their extensive experience of managing project of this nature. They have also used their network of contacts to help us get in touch with the people needed during the different phases of this project.
Lund University	The Faculty of Engineering LTH at Lund University has provided this project with the needed computer software, along with access to various workshops.
Uniti Sweden AB	Uniti (a pioneering electric car start-up) has provided this project with carbon fiber. They have also provided access to their facilities to paint and assemble the dinghy.
GT Prototyper	Provided a 3D printed part.
Malmö Segelsällskap	Provided the rib boat used during the testing.
Nils Malmgren	Provided the epoxy.
Scott Bader	Provided the composite glue.

The following persons contributed to the project:

Nils Bjerkås	Our supervisor from Essiq AB. Nils is head of Essiq:s office in Malmö and has extensive experience of sailing due to several years in the world match racing tour. Nils was of great assistance while evaluating concepts and developing technical solutions.
Johan Revstedt	Our supervisor from Lund University. Johan is professor in fluid dynamics and was of great help, especially during the CFD simulations.

Oscar Wiberg	Mechanical engineer at Corebon AB. Has an extensive experience working with carbon fiber. The prototype would probably look very different if Oscar did not gladly spend countless hours with us in the workshop.
Mikael Häll	Temporary supervisor from Essiq AB.
Curt Hallberg	Engineer at Essiq AB. Gave us access to his workshop for all the carbon fiber work. He also provided with a lot of creative and useful ideas.
Svante Bouvin	Metal workshop.
David Eriksson	Wood workshop.
Josef Forslund	CNC milling.
Johanna Johansson	Report advisor.
Tove Jungenfelt	Sticker applicator.
Lars-Åke Karlsson	Washer manufacturer.
Peder Karlsson	Wood workshop.
Axel Urde	Art consultant. Responsible for designing and painting the pattern of the hull.
Ulla Urde	Academic Support Centre.
Ryszard Wierzbicki	Metal workshop.

Lund, January 2018

Simon Karlsson and Jesper Urde

Table of contents

List of acronyms and abbreviations

α	angle of attack
α_f	flap angle
ρ	density
Λ	sweep angle
AR	aspect ratio
b	wingspan
Center of effort	the resultant of all the forces
Cd	drag coefficient
Chord	a straight line between the leading edge and the trailing edge of an airfoil
Cl	lift coefficient
Displacement mode	sailing while not foiling
D	drag
L	lift
L_{cb}	the lift generated by the centerboard-foil
L_r	the lift generated by the rudder-foil
Ride height	the distance between the hull and the surface of the water
Stagnation point	a point in a flow were the velocity is zero
Stall angle	the angle of attack causing an abrupt loss of lift
Strut	the vertical wings of the hydrofoils
TR	taper ratio
U	velocity

1 Introduction

This chapter provides a description of the purpose of this thesis work and a short introduction to hydrofoiling.

1.1 Background and purpose

Today hydrofoiling sailboats, boats with submerged wings attached underneath their hulls, making the boat fly above the water surface, are extremely popular. However, dinghies purposely built to hydrofoil are all very expensive. To reduce the cost for the consumer, one alternative could be to build separate hydrofoils, which can be attached to a regular, inexpensive, non-foiling, dinghy. This was the idea that lead to this project. The Europe dinghy, which is described more in detail below, is a common and cheap single sail, one-person dinghy. When comparing the prices of top-of-the-line purpose-built hydrofoiling dinghies with the prices of regular Europe-dinghies it is obvious that potential cost savings can be made here. See Appendix A for a comparison of typical price differences.

The aim of the project was thus to investigate if a Europe-dinghy could be complemented with separate hydrofoils in a simple and practical manner. Therefore, the main goal of the project was to build and test a prototype, as a proof of concept. This could then, at a later stage (after the thesis work was completed), eventually lead to a real product.

Research question: Can a Europe-dinghy be provided with separate hydrofoils in a practical manner?

This main question can be divided into several smaller questions:

- How can the hydrofoils be fitted to the hull of a Europe-dinghy in a rigid manner, while still being detachable and without making any permanent changes to the boat?
- Is the hull of a Europe-dinghy able to withstand the increased forces caused during hydrofoiling without additional reinforcements?
- Can a Europe-dinghy achieve hydrofoiling while using hydrofoils that are detachable and without making any permanent changes to the boat?
- Can an active control system of the hydrofoils be designed to provide a stable flight during hydrofoiling?

1.2 Hydrofoiling: an introduction

Hydrofoils are horizontal wings attached to a boat under the water surface. When the boat reaches a certain threshold speed, the lift generated from these wings – or foils – will be sufficient enough to lift the hull out of the water, leaving only the foils submerged. This results in a significantly smaller wetted surface area for the boat, which reduces the water resistance, and thereby increases the speed.

The first ever successful hydrofoiling boat was developed by Alexander Graham Bell and his wife, Mabel Bell, in the early 20th century. This vessel was called the *Hydrodrome* and could reach velocities up to 60 knots [1]. The Hydrodrome can be seen in Figure 1.1.

Figure 1.1 The Hydrodrome [2].

The concept of hydrofoiling was developed and used on a variety of vessels, from surfboards to passenger ferries and military boats. However, only in 2013, when hydrofoils were introduced in the famous sailing competition *America's Cup*, did the interest for hydrofoiling really explode [3]. In Figure 1.2, a foiling catamaran used in Americas Cup is shown. Since then, a number of high tech, purpose built, foiling sailing dinghies has reached the market.

Figure 1.2 A hydrofoiling catamaran used in Americas Cup [4].

1.3 The Europe-dinghy

In the 1930s, the dinghy class referred to as the Moth was introduced. This was a construction class, which means that individuals could design their own dinghies within a few simple rules regarding the length of the hull, the sail area, etc. The Europe-dinghy was designed in 1963 as a one-design dinghy under the Moth rule.

The Europe-dinghy grew fast in popularity and became a class of its own. It was an Olympic class for several Olympics and is today one of the most common sailing dinghies worldwide.

Since the Europe-dinghy is a common, affordable dinghy, it was thought to be a good choice of a dinghy that could be converted to a cheap foiling dinghy for the masses [5]. A modern Europe-dinghy is shown in Figure 1.3.

Figure 1.3 A Europe-dinghy.

Basic measurements of a Europe-dinghy are presented below [5]:

- Length: 3.35 meter
- Width: 1.38 meter
- Hull weight: 45 kilograms

1.4 Essiq AB

Essiq is an engineering consulting company founded in 2005. Since the start, their workforce has increased to 250 employees working with product development within the four competence areas of Design & UX, Mechanics, Project Management and Software & Electronics. Essiq already had a strong connection to sailing, thanks to their own team at the M32 circuit - a competition for high performance catamarans [6].

Essiq immediately showed interest when presented with the idea of this master thesis and has supported the project from the start. Apart from financial support, they offered expertise and guidance regarding planning and management of projects of this nature. Using their network of contacts, Essiq also provided connections to people with the necessary skills required during the different phases of this project.

2 Theory

The theory used as a foundation for this project will be presented in this chapter. The physics behind sailing and hydrofoiling is in large extension based on basic wing theory. Therefore, basic wing theory will be the starting point.

2.1 Basic wing theory

To understand how hydrofoils work, it is essential to first review some basic wing theory.

2.1.1 **Airfoil nomenclature**

Typical airfoil nomenclature can be seen in Figure 2.1 below.

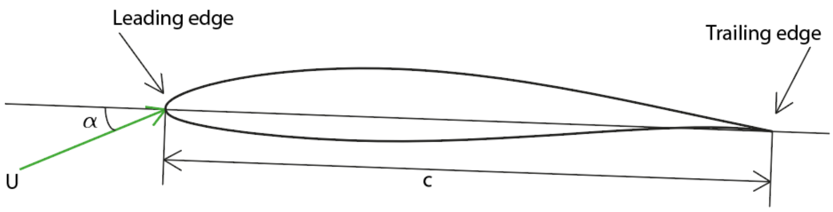

Figure 2.1 Airfoil nomenclature.

As can be seen in the figure above, the foremost edge and the rearmost edge of the airfoil are referred to the leading edge and the trailing, respectively. The chord line is the straight line between the leading and trailing edge. The length of the chord line is called the chord, and is denoted *c* [7, p. 250].

Another relevant term is the angle of attack, α, i.e. the angle between the chord line and the oncoming flow [7, p. 17].

2.1.2 **Wing planform**

The planform of the wing is the silhouette of the wing when viewed from above, see Figure 2.2 below.

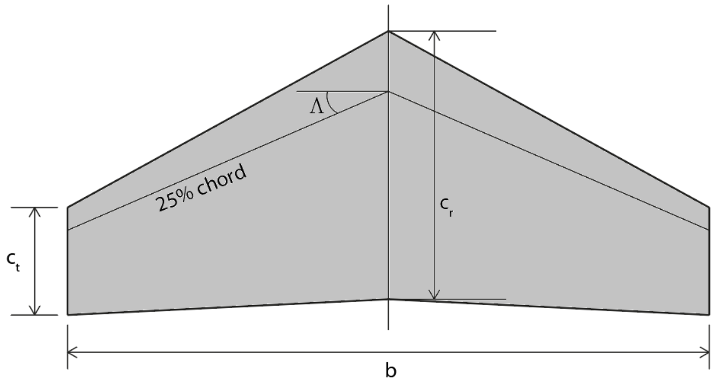

Figure 2.2 The planform of a wing.

A few relevant notations are used to define the planform of a wing. The image above shows that the wing has varying lengths of the chord at the root, c_r, and at the wing tips, c_t. The mean chord, $\bar{c}$, is defined as:

$$\bar{c} = \frac{(c_r + c_t)}{2} \tag{2.1}$$

Another central notion is the aspect ratio, *AR*. The aspect ratio describes the ratio between the wingspan, *b*, and the mean chord, and is defined as:

$$AR = \frac{b}{\bar{c}} = \frac{b^2}{A} \tag{2.2}$$

The ratio between c_r and c_t is referred to as the taper ratio, *TR*:

$$TR = \frac{c_t}{c_r} \tag{2.3}$$

It is common that wings are not entirely straight, but have a certain sweep angle, Λ, which can also be seen in the Figure 2.2. The sweep angle is defined as the angle of the 25% chord from the leading edge relative to a line that is perpendicular to the centerline of the aircraft [8, p. 109], [9].

There is a relation between the optimal sweep angle and the taper ratio. From *Principles of Yacht Design, Fourth Edition*, by Larsson, Eliasson and Orych, the following diagram, displaying the relation between the two parameters, can be found [8, p. 114]. See figure 2.3:

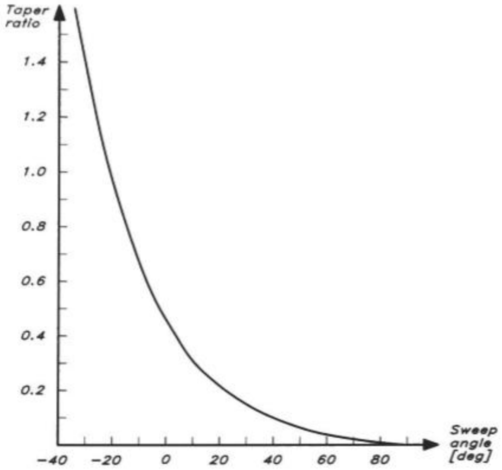

Figure 2.3 The relation between the sweep angle and the taper ratio [8, p. 114].

In Figure 2.4 below, the front view of a pair of wings is shown. The angle between the horizontal line and the wings is called the dihedral angle [9].

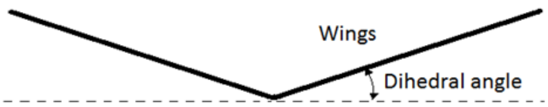

Figure 2.4 Definition of the dihedral angle.

2.1.3 **The forces acting on a wing**

When a solid object is moving through a fluid, a force is exerted on it. The component of the force that is perpendicular to the flow direction is called lift. A typical example of this is a regular airplane, using airfoils in order to fly in the air. In water, hydrofoils generate lift exactly the same way. However, the fluids create different settings for the foils [10].

To explain how hydro- or airfoils generate lift and what forces are involved during flight, an airplane can be used as an example. Figure 2.5 provides a clear description of which forces are acting on a regular airplane.

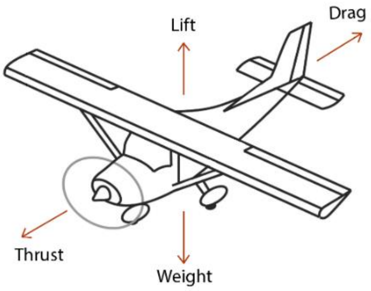

Figure 2.5 The forces acting on an airplane during flight.

Two important forces appear: *Lift (L)* and *drag (D)*. Lift is directed perpendicular to the direction of the flow and opposes the weight of the airplane, keeping the airplane flying [10]. Drag is the force directed in the opposite direction of the movement of the airplane, slowing the airplane down, requiring thrust to counteract [11].

2.1.4 **How lift is generated**

Two popular theories are used to explain how lift is generated:

The Coanda effect describes how the flow of a fluid is attracted to the surface of a solid object [12]. Thanks to this effect, a fluid flowing around a wing will follow the surface of the wing and be redirected. According to *Newton's third law*, this redirection of the fluid will result in an equal and opposite reaction – lift. It is important to note that both sides of the airfoil are contributing to the turning of the flow. If you neglect the redirection done by the upper surface, the theory would not be correct [10].

You can also calculate the amount of lift generated by a wing using Bernoulli's equation. This equation relates the local pressure to the local velocity in a fluid; if the velocity increases, the pressure decreases and vice versa. Thanks to the geometry of an airfoil, the air moves faster at the upper surface than the lower surface, thus a low pressure zone appears here, see Figure 2.6 below. By summarizing all the local pressures and multiplying them with the area over the entire surface of the wing, the lift force is given as the force that is perpendicular to the oncoming flow [13].

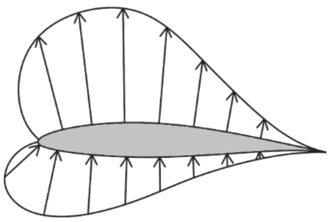

Figure 2.6 Typical pressure distribution for a lifting wing.

The two theories presented above both correctly explain some of the phenomena that creates lift. The full explanation, however, is complex and requires that both the downward deflection of the flow and pressure differences are taken into consideration. In this report, however, this will not be discussed any further.

2.1.5 Aerodynamic properties

In this section, a few important properties associated with aerodynamics will be explained.

Reynolds number is a dimensionless number that describes the ratio between inertia forces and viscous forces in a flow. This is a commonly used parameter in aerodynamics, and is defined as:

$$Re = \frac{\rho_\infty U_\infty L}{\mu_\infty} \tag{2.4}$$

Where ρ is the density, μ the dynamic viscosity, U is the velocity of the fluid with respect to the object and L is the characteristic length of the object [7, p. 38].

A point in a flow where $U = 0$ is referred to as a *stagnation* point. As described in section 2.1.4, the pressure will increase when the speed is decreased. A high-pressure zone is therefore expected around a stagnation point. An airfoil is known for having a stagnation point at the leading edge [7, p. 255].

The better the flow follows the surface of the wing, the more efficient the wing becomes. When the angle of attack increases, one effect might also be that the flow starts to separate from the wing, beginning at the upper surface of the trailing edge. Increasing the angle of attack will encourage further separation, until the point where the wing abruptly loses significant amounts of lift. This is known as the *stall-angle*, and is shown in Figure 2.7 [14].

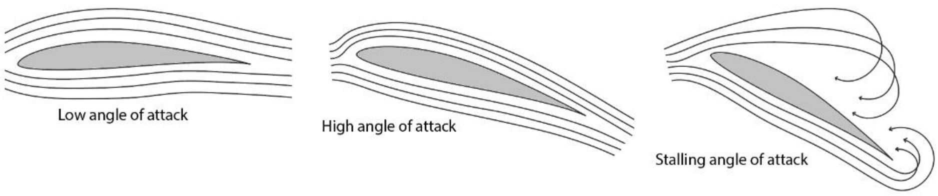

Figure 2.7 Stall angle explained.

Pressure differences across the surfaces of a wing will cause spillage around the wing tips, from the bottom surface to the top surface. This creates a wing tip vortex that presses down on the wing somewhat. This is referred to as *downwash*. To compensate for this loss of lift, a higher angle of attack has to be used. The addition to the angle of attack caused by the downwash is called the *induced angle of attack* [15].

2.1.6 **Factors affecting the lifting force**

There are numbers of factors that affect the amount of lift and drag a wing produces. For a wing moving through a fluid, the following factors can affect the lift:

The angle that the airfoil has versus the oncoming flow - the angle of attack - is of importance when turning the flow and producing lift. A higher angle of attack generates more lift, until the stall angle is reached. However, a higher angle of attack also generates more drag force, slowing the aircraft down [16].

The shape of the airfoil is of importance when generating lift. There are symmetrical and asymmetrical airfoils. Symmetrical airfoils generate no lift at a 0^{o} angle of attack, and asymmetrical airfoils do. In Figure 2.8 below you can see a symmetrical (to the left) and asymmetrical (to the right) airfoil [17].

Figure 2.8 A symmetrical airfoil to the left, and an asymmetrical airfoil to the right.

The planform of the entire wing also has an effect; the shape of the wings planform affects the amount of lift generated. An elliptic force distribution is favorable. This can for example be achieved by having tapered wings. In *Principles of Yacht Design, Fourth Edition*, by Larsson, Eliasson and Orych, the following diagram, showing the effect that the *TR* has on the drag, is presented [8, pp. 108, 114]. See Figure 2.9. A larger total area of the wing will of course also produce more lift.

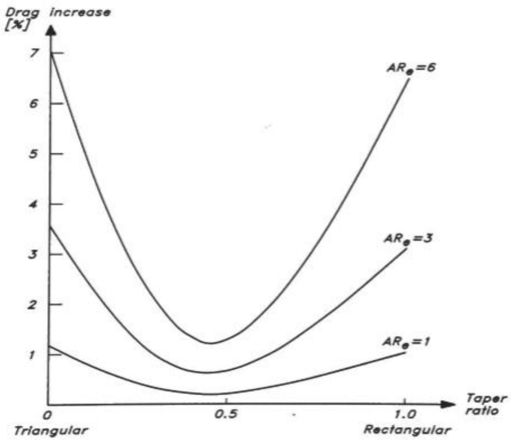

Figure 2.9 Taper ratio vs drag [8, p. 114].

Another factor that affects the lift is the velocity. Increasing the velocity of the flow relative to the airfoil will increase the lift [16].

Generally, the factors increasing lift will simultaneously increase the drag. The ratio between lift and drag, *L/D*, is important, since it can be used as a measure of how efficient a wing is. A higher *L/D-ratio* means that the wing can generate as much lift as possible to the cost of as low drag as possible. The aspect ratio can also be connected to efficiency of a wing. A large *AR* means that the wings will generate a higher *L/D-ratio*.

To better be able to compare lift and drag for different profiles, the *lift coefficient (Cl)* and *drag coefficient (Cd)* are often used. These are dimensionless coefficients that do not take the size of the wing into account, and relate the same way as the *L/D-ratio* does [18].

2.1.7 **Regulating the amount of lift**

It is important for any airplane to have the ability to change the amount of lift the wings are generating throughout the flight. This can be controlled in several ways by changing one or more of the factors affecting the lift described above. One of the most common solutions, however, is to make a part of the trailing edge of the airfoil movable, see Figure 2.10. This part is known as the *flap*. By rotating the flap downwards, the angle of attack of the entire wing effectively increases, resulting in more lift. Consequently, by turning the flap upwards, the effective angle of attack is decreased, resulting in less lift [19].

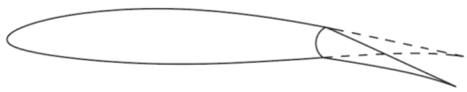

Figure 2.10 An airfoil provided with a flap.

Rotating the flap at the 30% chord a certain number of degrees will only be 45% as efficient as changing the angle of the entire airfoil the same number of degrees. In other words, if the angle of attack of the entire foil is $\alpha = 1^o$, the flap angle would have to be $\alpha_f = 2.2^o$ for the same effect to take place [20].

2.1.8 **Aerodynamic equations**

The equation for calculating the lifting force, *L*, can be written as:

$$L = C_L^{3D} * A * q_\infty \qquad (2.5)$$

Where q_∞ is the dynamical pressure, which can be expressed as:

$$q_\infty = \frac{1}{2}\rho_\infty * U_\infty^2 \qquad (2.6)$$

Here, ρ_∞ is the density of the fluid, A is the area of the wing, and U_∞ is the velocity [7, p. 20].

C_L^{3D} is the lift coefficient for the 3D case. This value can be calculated from the 2D lift coefficient as follows [21]:

$$C_L^{3D} = \frac{C_L^{2D}}{1+\frac{2}{AR}} \qquad (2.7)$$

2.2 Forces acting on a traditional sailboat

To understand the forces acting on a sailboat while foiling, it is preferable to understand the forces that propel a traditional, non-foiling, sailboat.

Since a sailboat moves in two elements – air and water – the boat will be affected by both aerodynamic and hydrodynamic forces, see Figure 2.11.

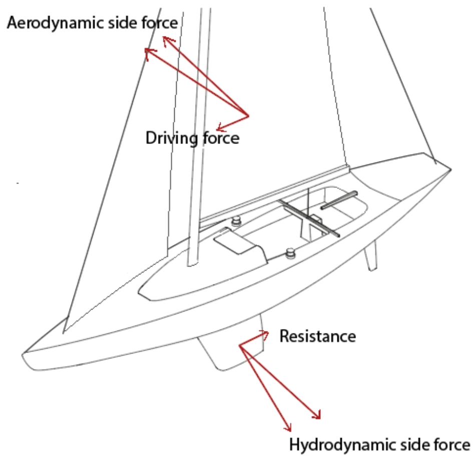

Figure 2.11 The forces acting on a boat while sailing.

The aerodynamic forces are acting on the sails, which propels the boat forward. The sail works in a similar manner as the wings of an airplane. When the wind hits the sail, the airflow will be redirected, and lift will be created[1]. However, this will also result in a side force, making the boat slide sideways. This force has to be cancelled out by a hydrodynamic force. Therefore, sailboats are equipped with a keel or centerboard, which compensates for this [8, p. 69].

---

[1] Note that the ”lift” generated by a sail is usually directed in the horizontal plane.

It is of utmost importance to make sure that the aerodynamic and hydrodynamic forces acting on a sailboat are in balance. A boat is said to be well balanced if it continues to travel in a straight line when the rudder is angled at zero degrees. If the boat is incorrectly set up, it will automatically try to turn either up or down against the wind, and the sailor will have to compensate with the rudder to keep a straight course. This is neither a very fast nor an efficient way to sail, since the rudder creates a lot of drag at a high angle of attack. To obtain a well-balanced boat, the resultant of the hydrodynamic forces should line up with the center of effort for the aerodynamic forces [8, p. 168]. This is shown in Figure 2.12.

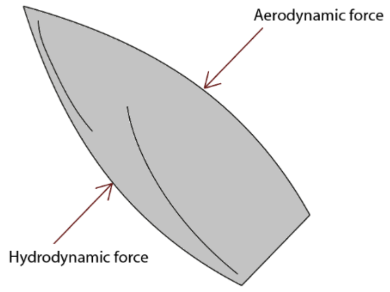

Figure 2.12 The lateral balance of a sailing boat.

2.3 Configuration of a foiling dinghy

The configuration of hydrofoils used in this project is the so-called T-foil. The dinghy is fitted with two hydrofoils: one main hydrofoil near the center of the boat, that produces the majority of the lift, and one aft hydrofoil near the stern of the boat that works as a stabilizer. Each of these hydrofoils have the appearance of the letter T turned upside down, hence the name. A typical foiling dinghy with this configuration is shown in Figure 2.13.

Figure 2.13 A widely used configuration for foiling dinghies [22].

There are other ways of arranging hydrofoils on a sailing dinghy, but this is the most common solution by far, and has been proven to work effectively.

In this configuration, each hydrofoil consists of two parts, one vertical and one horizontal. The vertical part, the *strut*, has the function of a traditional centerboard or rudder, i.e. to create a lateral resistance to make the boat sail in a straight line and preventing it from slipping sideways. This part should have a section of a symmetrical airfoil, to minimize drag and create a lateral lift force, to increase the ability of the boat to sail upwind.

The horizontal part, the *foil*, is the part that creates the lifting force that makes the boat “fly” over the water. The foil works in a similar fashion as the wings do on an aircraft, and should have the section of an asymmetrical airfoil to generate the maximum amount of lift.

The mutual relationship between the depth of the rudder and centerboard is of importance. If the rudder is too deep it might end up directly in the downwash of the centerboard foil, thus the rudder foil would be a lot less efficient. The danger of having a to short rudder is that it will lose control earlier than the centerboard while foiling too high, which then makes the boat impossible to maneuver. Some sort of golden mean is thus preferred.

As for an airplane, it is necessary for a foiling dinghy to have the ability of controlling the amount of lift generated by the foils. A crucial factor for successful foiling during longer periods of time is to obtain a stable and controlled flight at a constant height above the water surface, the so-called *ride height*. This is guaranteed by keeping the lifting force constant at all times. Since the lifting force is dependent of the velocity the dinghy travels with, the angle of attack of the foils must be adjusted constantly to compensate for the variations in velocity. As stated in section 2.1.7, this can be done by using a flap. This is a delicate operation, which means that an automatic control system of the flap is favorable [23].

2.4 Forces acting on a foiling boat

The aero- and hydrodynamic forces acting on a non-foiling boat described above also apply to a foiling boat. However, for the foiling boat, additional submerged horizontal wings are used. When the boat moves forward, these wings will generate a lifting force. When moving fast enough, this force will be able to lift the entire hull out of the water.

To obtain balance during foiling, it is important to make sure that the lifting force is distributed correctly between the main centerboard foil, and rudder foil. The goal is to have the resultant of the lifting force lining up with the center of gravity of the boat, as seen in Figure 2.14. Any deviations here will cause the boat to foil either in a nose-up, or nose-down configuration [23].

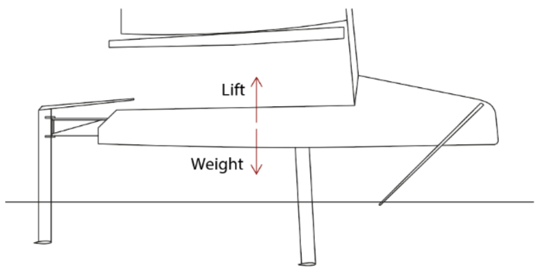

Figure 2.14 Balanced foiling on a typical foiling dinghy.

2.5 Ventilation and cavitation

By changing the angle of attack of the foils, the sailor can control the amount of lift that the foils produce, which in turn affects the ride height. By foiling higher, less area of the foil will be submerged and even greater speeds can be reached. However, by riding too high, the risk of *ventilation* increases. Ventilation occurs when the foils are close enough to the water surface for air to get sucked down to the lifting surfaces. This results in an abrupt loss of lift, and most likely in a spectacular crash [24, p. 208].

As explained previously in section 2.1.4, the pressure will decrease at the upper surface of a wing. When the wing is moving fast enough, the pressure will be reduced enough for the water close to the wing to start "boiling" (water evaporates earlier at lower pressure). This phenomenon is called *cavitation*. When cavitation occurs, the ability of the wings to produce lift is significantly reduced. There is also a risk of the wings being damaged by the condensation of the bubbles that occur during the cavitation. The aim of this project was not to optimize the hydrofoils for high top speeds. Therefore, cavitation was not predicted to be a major issue that would need to be considered during the design phase [24, p. 169].

3 Method

In this chapter, the method used during this master thesis is described.

The approach of this project was inspired by the product development and design methodology developed by Ulrich and Eppinger [25], and is presented in Figure 3.1 below:

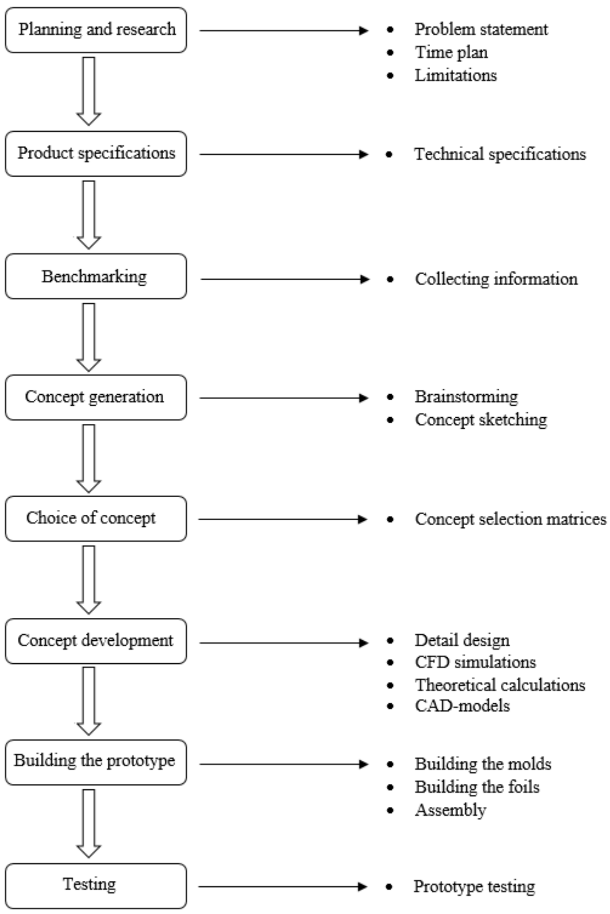

Figure 3.1 Overview of the method used during this project.

The different stages of this method will be described briefly under headings 3.1 to 3.8 below. A more thorough description of each stage will be presented in the subsequent chapters.

3.1 Planning and research

During the first stage of the project, the problem statement was formulated. Thereafter, a time plan was made. Initial research was also carried out. Based on the time plan and research, limitations for the project could be formulated.

3.2 Product specifications

The product specifications were set based on which criteria the prototype should fulfill. These specifications were weighted differently based on how important they were thought to be. This way, the concepts could easily be evaluated according to how well they fulfilled the specifications.

The main task of developing separate hydrofoils for a Europe-dinghy was split into three sub-categories to make the whole project more manageable, see Figure 3.2. Product specifications were thus stipulated for each of these sub-categories, respectively.

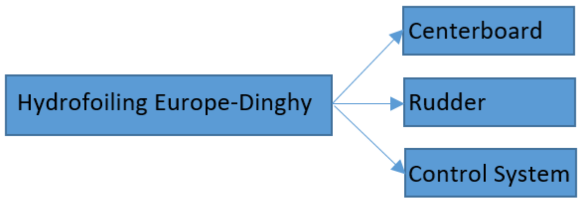

Figure 3.2 The three sub-categories of the main problem.

3.3 Benchmarking

During this stage, information concerning already existing foiling dinghies was gathered. Focus was especially set on the dimensions of the foils and their corresponding wing profiles. Although, the general configurations of different dinghies and their control systems were also observed.

The benchmarking was carried out, both by researching articles on the internet, and by studying physical foiling dinghies.

3.4 Concept generation

During this stage, concepts were generated for each of the three sub-categories specified above – centerboard, rudder and control system. Sketches were drawn to visualize the different concepts that would fulfill the product specifications.

3.5 Choice of concept

The different concepts were evaluated using concept selection matrices. Each concept received a score based on how well it fulfilled the weighted product specifications. The concept that got the highest score in respective sub-category was chosen.

3.6 Concept development

During this stage, the chosen concepts were further developed in detail. Simulations of different airfoils were carried out, using both XFOIL and ANSYS Fluent, to study which would be most suitable for this project. Based on the data from these simulations, the necessary dimensions of the foils could be calculated. The final design was chosen with regards to both the calculations, and the information gathered during the benchmarking.

The final design was thereafter created as a 3D CAD model using Creo Parametric.

3.7 Building the prototype

The foils were built out of carbon fiber, using the vacuum infusion process. The first step of the building process was to design female molds of the hydrofoils in CAD. These molds were thereafter hollowed using CNC milling. Carbon fiber weave was then laid out in different layers and orientations in the molds, which were later injected with epoxy plastic. The purpose of the epoxy was basically to work as a homogeneous and monolithic material in which the carbon fibers were embedded. During this part of the building process, a carbon fiber expert, Oscar Wiberg, mechanical engineer at Corebon AB [26], was consulted. Since the foils were built in halves they finally had to be glued together.

3.8 Testing

Testing of the hydrofoils were carried out at sea, to the west of Limhamn, Malmö, December 21. The authors took turns testing the boat, while the crew of a rib boat documented the test with photos and video.

4 Limitations

In this chapter, the limitations set for this project are summarized.

Since this was a fairly extensive project to be carried out during a relatively short period of time, some limitations had to be made. Therefore, instead of developing a finished product, only a prototype was made. This prototype was then to be used as a proof of concept, to show if a Europe-dinghy could be fitted with separate hydrofoils in a practical manner or not. This means that a number of additional limitations could be applied:

- Only one prototype was made. Given more time, additional, improved, prototypes should probably have been created. However, as stated before, during the scope of this project, there was only deemed time enough for one prototype to be made.
- No small-scale testing was carried out. Only computer-based simulations in various CFD software were used to generate the data required. Intrinsically, the simulations would need to be backed up by empirical data.
- No formal quantified market survey was carried out. The study was instead based on the observation that (A) foiling in international sailing is trending, (B) the sales of foiling dinghies (such as the Moth) is increasing and (C) there could be a market opportunity here, since there seems to be a demand for low-cost foiling dinghies.
- Cost efficiency has not been optimized. Rather, the highest quality materials were used for the prototype. This would of course be optimized for a real product, at a later stage. However, at this stage material failure should ideally be ruled out as a source of error.
- Simulating the forces acting on a boat while foiling is very complex, and was not done during this project. The amount of material used while building the prototype was entirely based on the experience from consulted experts.

5 Product specifications

In this section, lists of product specifications will be presented. In the product specifications, all factors that were thought to be of importance for a finished product was collected.

The specifications were weighted depending on how important each factor was thought to be. In this thesis work, the goal was, as stated in the introduction, only to build a prototype to be used as a proof of concept. Therefore, some of the factors that would be crucial for a finished product, like user friendliness, has been weighted low, and other factors, that are not as necessary for a finished product but important for the prototype, like having the ability to change settings, was weighted high for the prototype.

Since the overall concept of creating “separate hydrofoils for a Europe-dinghy” was quite a complicated and comprehensive concept, it was divided into three smaller sub-concepts: the centerboard, the rudder, and the control system, see Figure 5.1.

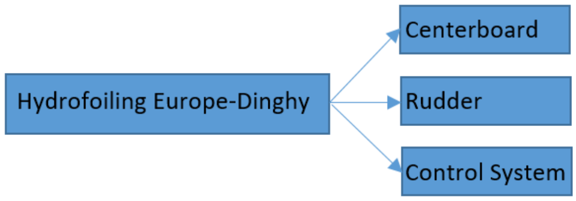

Figure 5.1 The three sub-concepts.

For each of these three areas, concepts would be generated, and the product specifications were weighted differently for each individual case.

The final product specification for each case are presented in detail in Appendix B.

6 Basic strength analysis of the hull

When fitted with hydrofoils, the hull of the Europe-dinghy would be exposed to forces it was not originally constructed for. As described in the product specifications, it was important to avoid any permanent changes or reinforcements to the hull. Therefore, a basic analysis was carried out to estimate if the hull could withstand the forces it would face during foiling.

The problem with this analysis was that the maximum forces occurring during foiling was unknown. The forces for the static case, when foiling along in a straight line can easily be estimated. However, it is not during the static case the maximum forces will occur. The critical forces will instead arise in the dynamic case, for instance during a high-speed crash. As stated in Chapter 4, these scenarios are far too complex to simulate during a project of this extent. Therefore, only some very basic calculations of the static scenario were made.

6.1 The static foiling case

The most critical factor was if the centerboard case would be able to withstand the forces. When a dinghy capsizes the sailor stands on the centerboard to right the boat again. From the authors own experience, it was known that a Europe-dinghy hull easily could withstand the forces corresponding to an 85-kilogram sailor standing on the tip of the centerboard. It was therefore interesting to compare this fact to the forces appearing during the static foiling case. The calculations that were made during this study are presented in Appendix C.

The conclusion drawn from the basic strength analysis was that the forces that occur at the centerboard case during static foiling is significantly less than the forces it is exposed to during righting from a capsize. Based on this, it was decided to carry on with the project, and let the final physical tests reveal if the hull can cope with the forces during more extreme dynamic load circumstances later.

7 Benchmarking

When developing a new product, a proven approach is to start by studying what is already on the market. Looking at what has already been done is a great way of learning from others and to gain inspiration.

Benchmarking was carried out to study what solutions similar products had used regarding the following subjects:

- Lifting areas of the foils vs the weight
- Area distribution between the main foil and the aft foil
- Which airfoils that were used
- Control systems

7.1 Existing foiling dinghies

A number of foiling dinghies in similar size to the Europe-dinghy was studied. Below follows a short description of these dinghies, which will later be referred to throughout the report.

7.1.1 **The Moth**

The Moth dinghy was the first dinghy that went foiling on a large scale worldwide. This is the most popular foiling dinghy today, attracting the best sailors in the world. This is a construction class, which means that the dinghies can be designed freely within a few simple rules. Consequently, it´s in the Moth class that the largest resources are spent on research and development, in the quest for the fastest design. This is the most extreme foiling dinghy today, and it represents the cutting edge of technology within this area [27].

7.1.2 **The Waszp**

The Waszp is a budget version of the Moth. It is a one-design class, which means that all Waszp dinghies look exactly the same. Since this dinghy uses less expensive and exotic materials, it is slightly heavier than the Moth, and is therefore slightly closer to the dimensions of the Europe-dinghy [28].

7.1.3 **The Foiling Laser**

The Laser is a traditional non-foiling dinghy that represents the absolute low-tech side of dinghy sailing. A company in Australia, called *Glide Free Foils*, has developed separate hydrofoils that can be attached to a standard Laser. The concept of this product is very similar to the idea behind this thesis project, which made this an interesting comparison [29].

7.1.4 **The Foiling Optimist**

In a project carried out by *Chalmers University of Technology* and *SSPA*, an Optimist dinghy was fitted with hydrofoils. During this project, a specially built Optimist was used, with permanent changes and reinforcements to the hull. This was of interest since the Optimist normally is a very slow dinghy. However, they were still able to make it hydrofoil [21].

7.2 Compilation of gathered information

In this section, the information found (and was deemed useful for this project) during the benchmarking is presented.

7.2.1 **Airfoils**

The different airfoils found during the benchmarking are presented here.

During the benchmarking, it was found that the following symmetrical airfoils had been used for the struts of the different foiling dinghies:

- NACA 63-012
- NACA 0012
- NACA 0009
- NACA 0015
- Eppler 297
- Eppler 836

It was also found that the majority of the foiling dinghies were using the same two asymmetrical airfoils for the foils.

- NACA 63-412
- Eppler 393

To increase the possibility of finding an optimal wingprofile for the foils, a few more profiles were studied. The website *www.airfoiltools.com* was used to find similar profiles to the ones listed above, and four more profiles with promising qualities were chosen [30].

- NACA 65-412
- NACA 64a-410
- Eppler 817
- Eppler 216

From the benchmarking phase it was noted that all of the centerboard foils that had a flap attached, had the flap connected at the 30 % chord from the trailing edge.

7.2.2 **Lifting areas of the foils vs weight**

It was of great value to compare the weight of the dinghies vs the lifting areas of their corresponding foils. Although several other factors do affect the ability to foil, this information was a good indication of what conclusions the other foiling dinghies had made regarding their design choices. The data gathered is shown in Table 7.1 below.

Table 7.1 Lifting areas vs weight for existing foiling dinghies [21], [23], [27], [28].

	Moth	***Waszp***	***The Foiling Optimist***	***The FoilingLaser***
Centerboard foil area [m^2]	0.100	0.124	0.220	0.160
Rudder foil area [m^2]	0.078	0.075	0.045	0.097
Total area [m^2]	0.178	0.199	0.265	0.257
Weight hull [kg]	15	25	35	59

7.2.3 **Centerboard and rudder depths**

Information was also gathered regarding the depths of the dinghies' centerboards and rudders. It was noted that the norm was to use approximately the same depth for the centerboards as for the rudders. See Table 7.2.

Table 7.2 Depths of the centerboard and rudder [21], [27].

Dinghy	***Centerboard depth [m]***	***Rudder depth [m]***
Moth	1.1	1
The foiling optimist	0.8	0.8

According to several reports, about 400 mm was a normal submergence depth of the struts while foiling [20], [21], [31].

7.2.4 **Control systems**

The majority of the dinghies studied during the benchmarking were using similar mechanical systems to automatically control the angle of attack during foiling. The most popular of these systems will be described below.

The main foil is fitted with a flap, which is mechanically linked to a so-called wand hanging from the bow of the dinghy, see Figure 7.1. This wand senses the ride height. If the dinghy is foiling at a low height, the wand will follow the surface of the water, and be angled backwards. The mechanical links will translate this rotation to a vertical motion that lowers the flap, increasing the lifting force. When the lifting force is increased, the ride height of the dinghy will also increase, which means that the wand will move forward. This will result in a smaller flap angle, decreasing the lifting force somewhat again. If designed correctly, this system will find an equilibrium and make sure that the dinghy rides at a constant height, regardless of the various velocities.

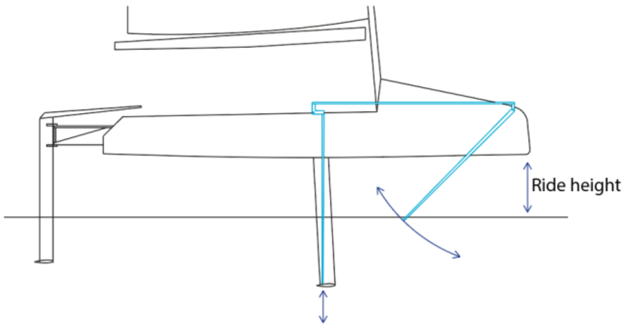

Figure 7.1 The control system of a Moth.

It is beneficial to have as long a distance as possible between the centerboard and the wand. A wand hanging from the bow will react for changes in the pitch (when the bow is moving either upwards or downwards), detecting and leveling out instabilities at an early stage. Modern moths today even have their wands hanging from bowsprits to further increase the offset between centerboard and wand, see Figure 7.2.

Figure 7.2 A moth with the wand fitted to a bowsprit [32].

It was found that one dinghy, the Foiling Laser, utilized a slightly different solution. Here, the wand was integrated directly in the centerboard, instead of hanging from the bow. It is still of course connected to the foil, changing the angle of attack mechanically. However, by having a shorter distance between the wand and the centerboard, the wand will not be able to detect the pitch; it will only sense the vertical distance to the water surface, resulting in an operational but somewhat less stable ride. This can be seen in Figure 7.3.

Figure 7.3 The foiling laser with the wand integrated in the centerboard [33].

The angle of attack could also be adjusted for the aft foil of the different dinghies that were studied. The trend was to use a solid rudder foil without a flap, and instead simply angle the entire rudder back and forth to change its angle of attack. This is done manually by the sailor.

8 Concept generation

A number of different concepts were evaluated during the project. As described in Chapter 5, the main concept was divided into three sub-categories: Centerboard, Rudder and Control system. Concepts for each of these were generated and are presented in this chapter.

There are a lot of ways to arrange hydrofoils on a sailing dinghy, but the most common solution by far, is the T-foil, which has been proven to work very effectively. Therefore, the decision to use this configuration was made at an early stage, and no other configurations were suggested. Furthermore, the fact that the Europe-dinghy already has been constructed to fit a central centerboard and an aft rudder at the stern, limited the possibilities for more imaginative solutions without modifying the hull of the dinghy.

The concepts regarding the centerboard and rudder therefore all have the T-foil as starting point.

8.1 Centerboard

The concepts for the centerboard focus on how to change the angle of attack of the foil. Four different solutions were suggested. These are presented below.

- *Flap with mechanical hinge*
  The foil is provided with a flap at the trailing edge, similar to the flaps on an airplane wing. This flap is connected to the main foil by a mechanical hinge, see Figure 8.1. This solution makes for an easily detachable flap. The downside is that there will be a gap between the foil and the flap that is not desirable from a hydrodynamic point of view. This is however a popular solution used by many foiling dinghies, like the Wazp.

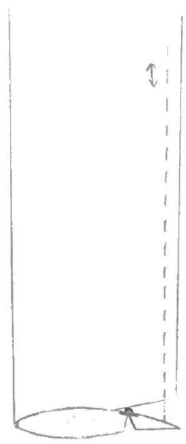

Figure 8.1 A flap with a mechanical hinge.

- *Flap with fiberglass hinge*
  Similar to the first concept, the foil is provided with a flap. The difference between this concept and the previous one, is that the hinge is constructed out of a thin strip of fiberglass stretching along the full wingspan of the foil. The flexibility of the fiberglass makes it possible to angle the flap up and down. This provides a much smoother transition between the foil and the flap, but is permanent and could potentially be fragile. This solution is widely used in the moth class and is shown as a sketch in Figure 8.2.

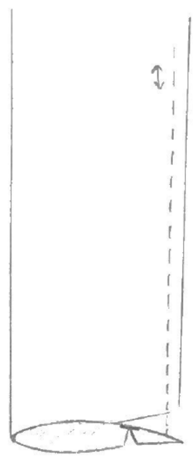

Figure 8.2 A flap with a fiberglass hinge.

- *Angle the entire foil*
  Another option was to angle the entire foil, see Figure 8.3. This solution is the best option from a hydrodynamic point of view, since the wingprofile is not "ruined" by a flap. A change of angle of the entire foil is more effective than a change of angle of the flap, which means that a smaller angle can be used. This results in less drag. However, there were concerns if this construction would be strong enough, since the hinge has a lot smaller area to be attached to. This solution has been used on the Foiling Laser described in section 7.1.3.

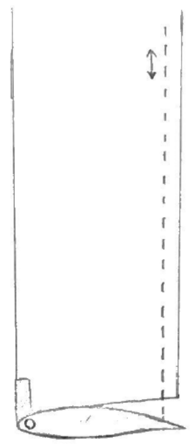

Figure 8.3 Angle the entire foil.

- *Angle the entire centerboard*
  In this concept, the entire centerboard and foil are fixed to each other, and the entire construction is angled back and forth to change the angle of attack. This solution is simple and strong; however, the lateral balance of the boat would be affected significantly when tilting the centerboard. No dinghies studied during the benchmarking used this solution. A sketch of this concept is shown in Figure 8.4.

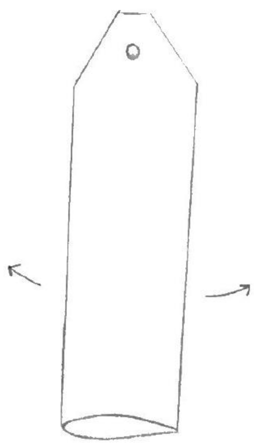

Figure 8.4 Angle the entire centerboard.

8.2 Rudder

As with the centerboard, the most important aspect of the rudder concept was how the angle of attack would be changed. The same four concepts developed for the centerboard were also used here.

- *Flap with mechanical hinge*
  The concept uses the same principles as the corresponding concept for the centerboard, and is shown in Figure 8.5.

Figure 8.5 A flap with a mechanical hinge.

- *Flap with fiberglass hinge*
  The concept also uses the same principles as the corresponding concept for the centerboard, and is shown in Figure 8.6.

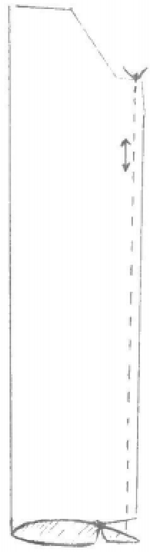

Figure 8.6 A flap with a fiberglass hinge.

- *Angle the entire foil manually*
  The concept uses the same principles as the corresponding concept for the centerboard. This solution has been used on the Foiling Laser and is shown in Figure 8.7.

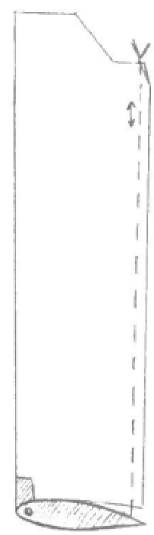

Figure 8.7 Angle the entire foil.

- *Angle the entire rudder manually*
  Just as for the centerboard, tilting the rudder will change the lateral balance of the boat. However, the rudder generally have a lot less area than the centerboard, and it is therefore not as crucial. Most modern foiling dinghies use this solution, since the advantages of having a strong and light rudder without moving parts is more important than the slight shift in balance. This concept is shown in Figure 8.8.

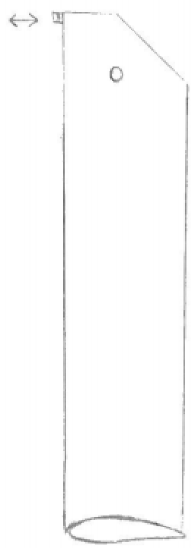

Figure 8.8 Angle the entire rudder.

8.3 Control System

The angle of attack of the centerboard foil is adjusted mechanically by a wand that senses the distance to the water surface. Two different systems were considered for the control mechanism.

- *Wand hanging from the bow*
  The wand would be more effective by having the ability to detect changes in pitch as well as ride height using this configuration. The downside would be that when using a boat not originally intended to foil, a more complicated construction would be required to connect the wand to the bow and translate the motion to the centerboard. This is the solution used most widely by purpose built hydrofoiling dinghies today. The concept is shown in Figure 8.9.

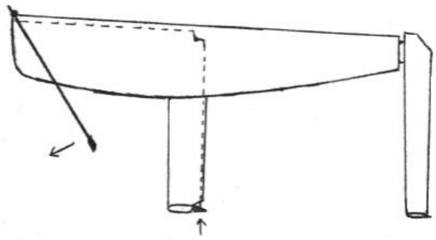

Figure 8.9 The wand hanging from the bow.

- *Wand integrated in the centerboard*
  In this concept, the wand is integrated directly in the centerboard. While not being as pitch-sensitive as the configuration described in the previous concept, this would be a far more simple and user friendly solution with fewer parts, see Figure 8.10.

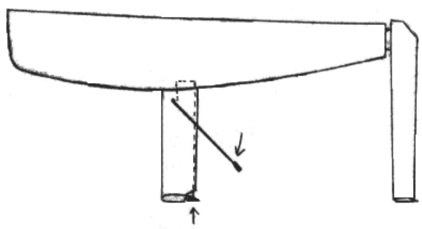

Figure 8.10 The wand integrated in the centerboard.

9 Choice of concepts

In this chapter, the method used to select the final concept is briefly described, and the final choices are presented.

To select final concepts for the centerboard, the rudder, and the control system, each of the concepts generated in Chapter 8 were graded on a scale from 1-5 for each of the product specifications that were developed in Chapter 5. The scoring was based on how well the concept were believed to satisfy the specifications, score 1 being the least- and 5 being the most eligible. The results from the selection were compiled in concept selection matrices, which are presented in Appendix D.

9.1 Final choice of concept

The final choices of concepts are motivated and presented below:

- Centerboard: The concept *"Flap with fiberglass hinge"* presented in section 8.1 was selected as the most promising configuration for the centerboard. The main advantages of this concept were its low technical complexity and that it would be easy to manufacture. Additionally, this concept would provide the smoothest transition between the main foil and the flap, which would benefit the performance of the dinghy. Thus, this concept received the highest score in the concept selection matrix, which can be seen in Appendix D, Table D.1. Considering the arguments previously stated above, and the fact that this configuration is known to be working well in the Moth class, the decision was made to choose this concept.
- Rudder: The concept *"Angle the entire rudder manually"* presented in section 8.2 was selected for the rudder. Similar to the centerboard, the main advantages of this concept were its low technical complexity and that it would be easy to manufacture. Unlike the centerboard however, the rudder did not need an automatic control system and would therefore benefit from being constructed as simple as possible with few moving parts. Therefore, this concept received the highest score in the concept selection matric seen in Appendix D, Table D.2. This was also a configuration known to be used

widely within the Moth class and were consequently chosen as the most promising option.

- Control system: The concept *"Wand integrated in the centerboard"*, described in section 8.3 was selected for the control system. Despite not being the best option performance-wise, this concept was considered to make up for it by being a much less complex construction that would be more user friendly. Once again, simple and easy foiling were prioritized above high performance. Therefore, this concept received the highest score in the concept selection matrix, seen in Appendix D, Table D.3. This is not the most common solution used among foiling dinghies, but it has been used successfully, for example by the foiling Laser.

10 Concept development

To develop and refine the concepts chosen in Chapter 9 more in detail, thorough calculations, simulations and drawings were made.

10.1 Preliminary selection of airfoils

To be able to rapidly and easily compare and evaluate the different airfoils found during the benchmarking, the program XFOIL was used. XFOIL was developed at *Massachusetts Institute of Technology*, and is used for the analysis and design of subsonic airfoils [34]. The results given from this program might not be as accurate as for a complete CFD analysis in a high-end simulation program, but provides a clear indication of the general performance of the airfoil. XFOIL though, is a lot faster and more straightforward than the top of the line simulation programs, which is why it was used as a first screening of the airfoils [35].

During the analysis in XFOIL, the *Cl* and *Cd* values for each airfoil were calculated for a number of angles of attack, α. With this data it was possible to calculate the *Cl/Cd-ratio* to compare the performance of the different foils.

The following airfoils were evaluated in XFOIL:

Symmetrical:

- NACA 63-012
- NACA 0012
- NACA 0009
- NACA 0015
- Eppler 297
- Eppler 836

Asymmetrical:

- NACA 63-412
- NACA 64a-410
- NACA 65-412
- Eppler 393
- Eppler 817

During the simulations, Reynolds number was necessary. In the case of an airfoil, the characteristic length, L, is the chord, c. Equation (2.4) can therefore be written as:

$$Re = \frac{\rho_\infty U_\infty c}{\mu_\infty} \tag{10.1}$$

The simulations were run with typical values for water at 20°. The density and dynamic viscosity were set to $\rho_\infty = 998.2\ kg/m^3$ and $\mu_\infty = 1.002 * 10^{-3} Pa * s$, respectively [36].

Thereafter a reasonable chord length was estimated to $c = 0.13\ m$ and the velocity was chosen to $U_\infty = 11\ knots = 5{,}66\ m/s$. The exact values of U_∞ and c were not critical, since they were only used to compare the different airfoils to each other under identical circumstances.

With the data described above, Reynolds number was given from Equation (10.1) as $Re = 733\ 000$.

The range of angles of attack started at $\alpha = -4^o$ with increments of 1° degree, until they did not converge anymore, which meant that they reached their respective stall angle. Furthermore, the number of iterations were set to 100 per angle of attack, and the Mach number was set to 0 for all simulations.

The *Cl/Cd-ratio* for the symmetrical airfoils are shown in Figure 10.1 below.

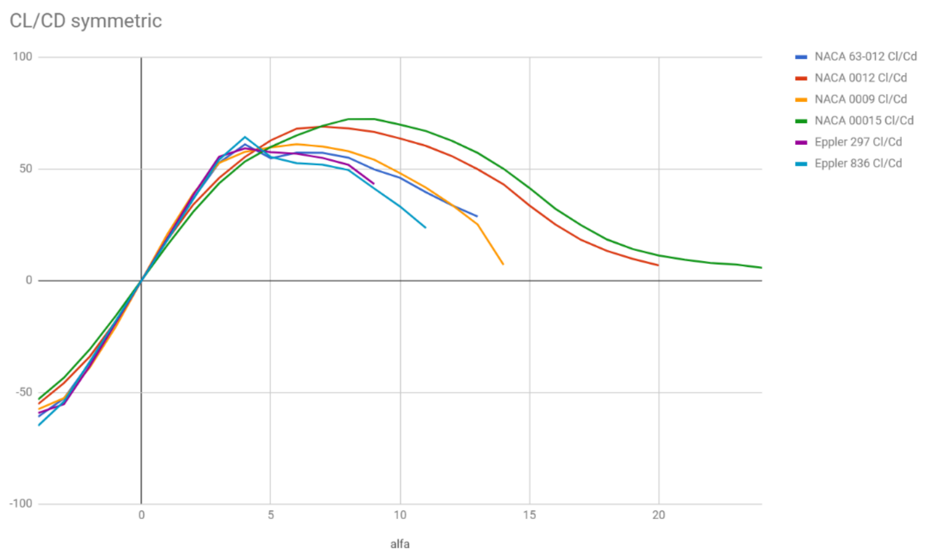

Figure 10.1 Cl/Cd for the symmetrical airfoils.

As can be seen in Figure 10.1, NACA 0012 and NACA 0015 had the best Cl/Cd ratio for the largest span of angles of attack. As discussed in Chapter 2.5, symmetric airfoils would be used for the struts of the rudder and centerboard. Thus, the choice of struts was now narrowed down to either NACA 0012 and NACA 0015. The final choice of airfoil for the struts will be presented in section 10.3.1.

The Cl/Cd for the asymmetrical airfoils are shown in Figure 10.2 below.

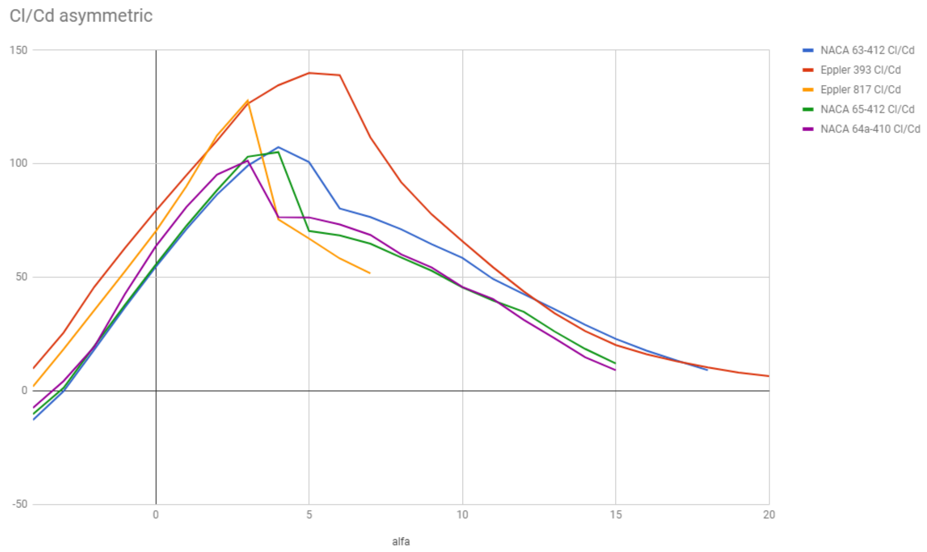

Figure 10.2 Cl/Cd for the asymmetrical airfoils.

As discussed in Chapter 2.5, asymmetrical airfoils would be used for the lifting foils. The two airfoils that seemed the most promising from the simulations were selected to be further evaluated. The Eppler 393 profile had by far the best *Cl/Cd-ratio*, and was chosen as one of the two profiles. The Eppler 817 also showed promise, but stalled earlier than desirable. Therefore, the NACA 63-412 was chosen as the other wingprofile to be further evaluated. NACA 63-412 has an even and smooth curve – not an abrupt end like the Eppler 817 – and is the next best option, considering the *Cl/Cd-ratio*.

10.2 Further evaluation of the lifting foils

To decide which of the two candidates for the lifting foils – Eppler 393 or NACA 63-412 – would be the most expedient, exploratory calculations, with data provided by XFOIL, were made. By evaluating the airfoils as if they would both be used in the final prototype, conclusions could be drawn regarding which would be the most suitable. Preliminary planform-areas required for takeoff speed and cruise speed during stable foiling was thus calculated. This would later be a solid basis when deciding which airfoil to finally use.

10.2.1 **Preliminary flap simulations**

There was a need to gather some additional data before the comparative calculations could continue.

As stated in section 9.2, it was decided that a flap would be used on the centerboard foil. To obtain the *Cl* and *Cd* values for Eppler 393 and NACA 63-412 with a flap, XFOIL was used once again.

During the simulations, the same Reynolds number, Mach number and number of iterations were used as before. The hinge location for the flap for both of the airfoils was set to 30% of the chord from the trailing edge.

Figure 10.3 below displays the *Cl/Cd* results for these two wing profiles with an angle of attack of $\alpha = 0^o$, but with varying flap angles of $\alpha_f = [-7^o..18^o]$.

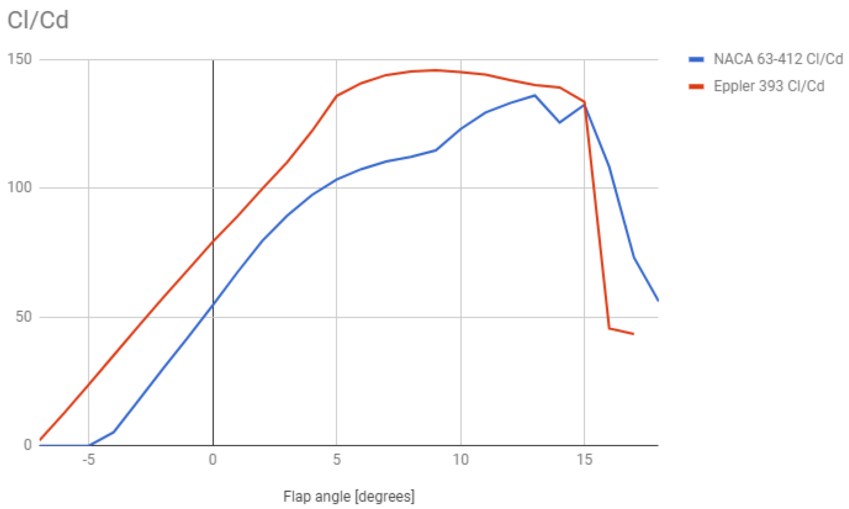

Figure 10.3 *Cl/Cd* for airfoils with a flap.

10.2.2 **Preliminary lifting areas**

As previously stated, to compare the Eppler 393 and NACA 63-412 airfoils to each other, the area required from each of them to get the boat to foil was investigated. This area could later be used to calculate the takeoff speed and cruise speed during foiling. The airfoil that had the best values here would then be selected.

The required lifting areas were decided based on two design principles:

(1) Foiling at “cruising speed”: When the boat already is foiling, less lift is needed from the foils. The foils should therefore be designed to operate with their lowest

amount of drag during this phase. The foils generate least amount of drag with a flap angle of 0^o. To calculate the exact cruising speed of a boat requires complex velocity prediction programs, which were not available during this project. The cruising speed was therefore instead simply estimated to 10 knots. The foils should therefore be designed to operate with a 0^o flap angle at 10 knots of boat speed.

(2) Takeoff: During the takeoff phase, when the boat is just about to start to foil, it seemed reasonable to design for the maximum amount of lift to the lowest amount of drag. In other words, at this point the foils should be working with their maximum *Cl/Cd-ratio*. Based on the product specifications, it was important to have a low takeoff speed. The aim was therefore to be able to start to foil in about 6-7 knots of boat speed, which is a velocity reached fairly easy in a Europe-dinghy in moderate wind strengths.

10.2.2.1 Distribution of the lifting force

To be able to calculate the lift required from the centerboard and rudder foils, the distribution of the lift force between the foils needed to be known. This could later be used to calculate the area needed for each wing, using either Eppler 393 or NACA 63-412. The vertical forces acting on a hydrofoiling dinghy are shown in Figure 10.4 below.

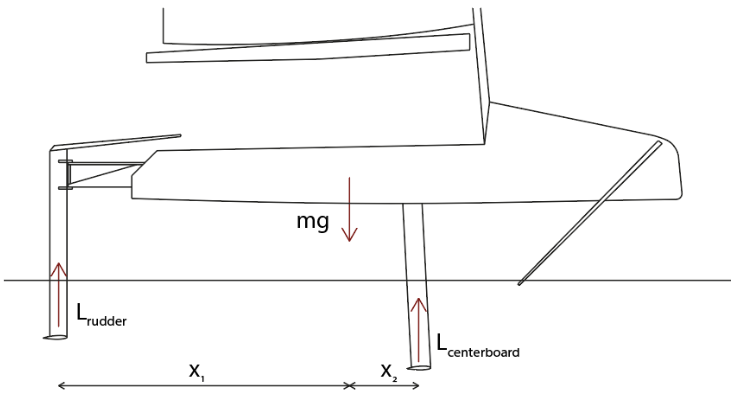

Figure 10.4 Distribution of the lift.

To obtain equilibrium, the following expression must be true:

$$L_{rudder} * x_1 = L_{centerboard} * x_2 \quad (10.2)$$

In this case, the weight of the sailor is greater than the entire weight of the boat, which means that she can easily alter the center of gravity significantly depending on where she sits. The intention was therefore to make sure that the distribution of the lifting force from the foils is such that the sailor can sit in a reasonable position, with the possibility of moving both forwards and backwards to adjust the balance of the boat if needed.

By measuring the Europe-dinghy, x_1 and x_2 was set to 1.12 meter and 0.48 meter, respectively.

The ratio between the lift from the rudder foil and lift from the centerboard foil should, based on Equation (10.2) be:

$$\frac{L_{centerboard}}{L_{rudder}} = \frac{x_1}{x_2} = \frac{1.12}{0.48} \approx 2.33 \tag{10.3}$$

By normalizing this ratio, it can be shown that the ratio between $L_{centerboard}$ and L_{rudder} was:

$$\frac{L_{centerboard}}{L_{rudder}} = \frac{0.7}{0.3} \approx 2.33 \tag{10.4}$$

The conclusion was, in other words, that 70% of the lift should be generated by the centerboard foil, and 30% should be generated by the rudder foil.

10.2.2.2 Calculating lifting areas

To design with regard to the cruising speed, the following expressions for calculating the length of the chord was derived. When the chord was known, the entire area of the foil could be calculated.

When the boat is foiling, the following expression is true:

$$L = mg \tag{10.5}$$

Equation (10.5) combined with Equation (2.5) and (2.6) gives:

$$mg = \frac{\rho}{2} C_L^{3D} U^2 A \tag{10.6}$$

When Equation (2.7) is inserted in Equation (10.6), the following expression is obtained:

$$mg = \frac{\rho}{2} \frac{C_L^{2D}}{1+\frac{2}{AR}} U^2 A \tag{10.7}$$

Using Equation (2.2), Equation (10.7) can be rewritten to:

$$mg = \frac{\rho}{2} \frac{C_L^{2D}}{1+\frac{2\bar{c}}{b}} U^2 b\bar{c} \tag{10.8}$$

This expression can be written as:

$$\bar{c} = \frac{b}{\frac{\rho}{2} C_L^{2D} U^2 b^2 \frac{1}{mg} - 2} \tag{10.9}$$

By separating Equation (10.9) into two, one for the centerboard and one for the rudder, their respective cords could be calculated.

$$\bar{c}_{cb} = \frac{b_{cb}}{\frac{\rho}{2} C_{L,cb}^{2D} U^2 b_{cb}^2 \frac{1}{mg_{cb}} - 2} \tag{10.10}$$

$$\bar{c}_r = \frac{b_r}{\frac{\rho}{2} C_{L,r}^{2D} U^2 b_r^2 \frac{1}{mgr} - 2} \tag{10.11}$$

When the areas of the foils were known (the mean chord times the wingspan), these could be used to calculate a corresponding takeoff speed, as shown below. The Lifting force gets a contribution from both the centerboard foil and rudder foil.

$$L = L_{cb} + L_r \tag{10.12}$$

Using this, combined with Equation (2.5) and (2.6) it is possible to write:

$$L_{cb} = \frac{\rho}{2} \frac{C_{L,cb}}{1 + \frac{2}{AR_{cb}}} U^2 A_{cb} \tag{10.13}$$

$$L_r = \frac{\rho}{2} \frac{C_{L,r}}{1 + \frac{2}{AR_r}} U^2 A_r \tag{10.14}$$

The total amount of lift required for takeoff is therefore:

$$mg = L = \frac{\rho}{2} \frac{C_{L,cb}}{1 + \frac{2}{AR_{cb}}} U^2 A_{cb} + \frac{\rho}{2} \frac{C_{L,r}}{1 + \frac{2}{AR_r}} U^2 A_r \tag{10.15}$$

From this expression, the velocity, U, can be derived to:

$$U = \left[\frac{2mg}{\rho} \left(\frac{C_{L,cb} A_{cb}}{1 + \frac{2}{AR_{cb}}} + \frac{C_{L,r} A_r}{1 + \frac{2}{AR_r}} \right)^{-1} \right]^{1/2} \tag{10.16}$$

To decide which wingprofile to use, some general input data combined with data from XFOIL was used in the expressions derived above.

The input data used in the formulas are presented below.

- ρ: The density of the water, set to 999,8 kg/m^3.
- b_{cb}: As explained in section 2.1.6, it is beneficial for the wingspan to be as wide as possible. However, for practical reasons, it was decided that the maximum wingspan should be limited by the width of the hull, 1.38 meter.
- b_r: The wingspan of the rudder was set to obtain a similar *AR* as for the centerboard foil.
- m: The mass of the hull of the Europe-dinghy is 45 kilograms. Fully equipped, it was estimated to weigh 60 kilograms. Added to that is a sailor of 80 kilograms. This resulted in a total mass of 140 kilograms.
- U: To calculate the exact speed of a boat requires complex velocity prediction programs, so-called VPPs. A program of this kind was not available during this project. The “cruising speed” was therefore simply estimated to 10 knots, based on experience from other foiling dinghies.

The relevant data received from XFOIL is presented in the Tables 10.1-10.2 below.

Table 10.1 Centerboard foil with flap.

Airfoil	*Cl at 0-degree flap*	*Cl at max Cl/Cd-ratio*
Eppler 393	0.543	1.210 (at 9 degrees)
NACA 63-412	0.342	1.284 (at 13 degrees)

Table 10.2 Rudder foil with no flap.

Airfoil	*Cl at 0-degrees*	*Cl at max Cl/Cd-ratio*
Eppler 393	0.543	1.090 (at 5 degrees)
NACA 63-412	0.342	0.790 (at 4 degrees)

When using the data from Table 10.1-10.2 as input in Equations (10.9), (10.10) and (10.15), the following results, which can be seen in Table 10.3, were obtained.

Table 10.3 Areas and takeoff speed for respective foil.

	Mean chord [mm]		*Area [m²]*		
Airfoil	*Centerboard*	*Rudder*	*Centerboard*	*Rudder*	*Takeoff speed [knot]*
Eppler 393	0.113	0.079	0.156	0.068	7.325
NACA 63-412	0.198	0.140	0.273	0.121	5.846

10.3 Choice of airfoils

In this section, the choices of airfoils are presented and motivated.

10.3.1 **Symmetrical airfoils**

As could be seen in section 10.1, the NACA 0012 and NACA 0015 showed significantly better *Cl/Cd-ratio* than the other symmetrical airfoils that were evaluated, for a wider range of angles of attack. The decision was finally made to use the NACA 0012 airfoil because of its *Cl/Cd-ratio* being better at lower angles of attack. This would be the most commonly occurring angles for the struts. Furthermore, considering that the NACA 0012 was the airfoil used by most of the dinghies studied during the benchmarking, the choice was made to use this profile.

10.3.2 **Asymmetrical airfoils**

For the asymmetrical airfoils, the NACA 63-412 was chosen, despite not having the highest *Cl/Cd-ratio*. The advantage of this profile was however its ability to generate a wide span of both high and low *Cl*-values. The Eppler 393 had consistent high *Cl*, which made it difficult to develop a design with the ability to initiate foiling at low speeds and at the same time be optimized for higher cruising foiling speeds.

When the Eppler 393 was designed with regard to foiling at cruising speed, it resulted in very small areas of the foils. These areas would therefore need a higher takeoff speed than the NACA 63-412, which can be seen in Table 10.3.

On the other hand, when the Eppler 393 was designed for takeoff at low speeds, the consequence was that the foils generated far too much lift when reaching higher speeds. This meant that, during these conditions, the foils would need to constantly operate with a negative flap angle in order to reduce the abundant lift, which would increase the drag.

Also, as for the symmetrical airfoils, the NACA 63-412 was the most widely used wingprofile by the foiling dinghies found during the benchmarking.

10.4 Further evaluation of NACA 63-412 using CFD

As stated in section 10.1, simulations in XFOIL are not as accurate as a complete CFD analysis in a state of the art simulation program. Thus, after the decision of which airfoils to use was made, further analyses of NACA 63-412 were carried out with CFD in 2D. The airfoil was simulated for different angles of attack, both with and without a flap. For each angle, the corresponding *Cl* values were saved. The appearance of each flow situation was also studied.

The symmetrical airfoil did not need any further simulations, since no calculations of the lateral lift were to be made.

The program used was ANSYS Fluent. Below, the different settings used for the simulations are explained.

10.4.1 **Geometry**

A 2D surface of the airfoil was created in Creo Parametric, using coordinates obtained from XFOIL. This airfoil was uploaded to ANSYS and placed in a rectangular domain (Rectangle A). This domain was 50 chords long and about 30 chords high. The distance from the airfoil to the upper edge of the rectangle was set to one meter to resemble the distance between a submerged foil to the surface of the water. Finally, the airfoil was surrounded by two additional rectangles (Rectangle B and C). The geometry can be seen in Figure 10.5.

- Rectangle A: The outer rectangle
- Rectangle B: The middle rectangle
- Rectangle C: The inner rectangle

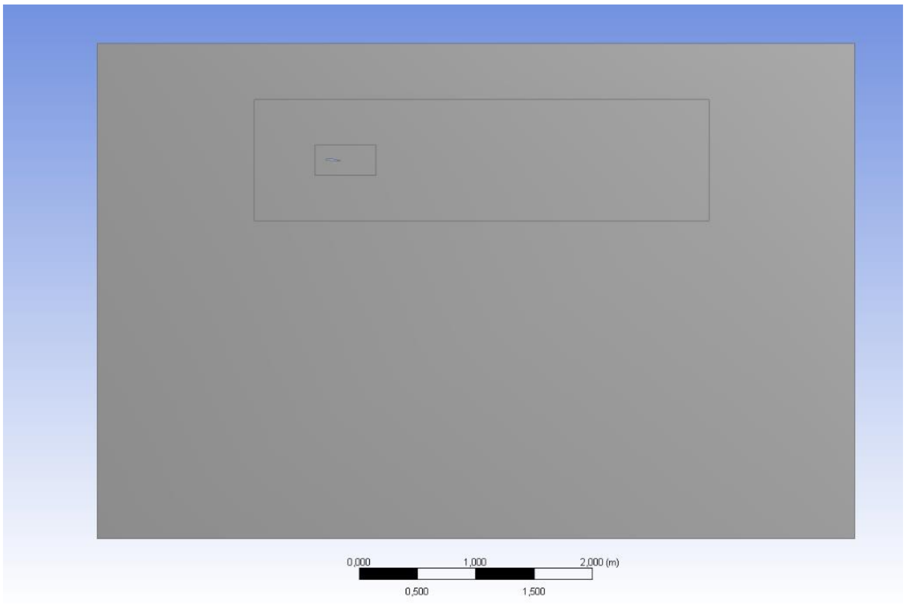

Figure 10.5 The geometry used in ANSYS.

10.4.2 **Mesh**

The quality of the mesh has a great impact on the results of the simulations. Generally, a finer mesh yields more accurate results, at the cost of longer simulation times. In this case, the most crucial areas of the simulation were the areas closest to the surface of the foil. Therefore, a very fine mesh was used close to the foil, and coarser meshes were used in the outer regions, far away.

Since several different angles of attack were to be simulated, one mesh had to be created for each individual angle.

Each rectangle was given a *face sizing*. By using this function, the elements in the rectangles closer to the center were made smaller, while a coarser mesh could be used for the outer rectangle. The resulting mesh is seen in Figure 10.6.

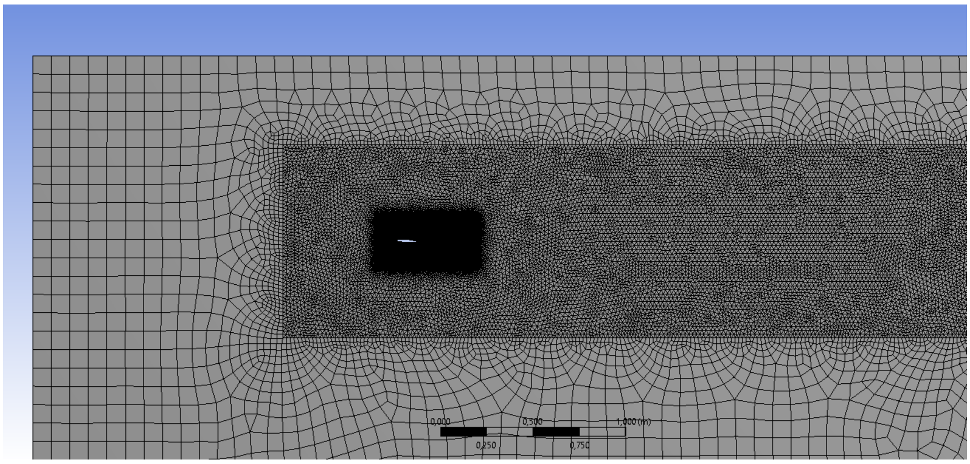

Figure 10.6 The mesh.

To further refine the mesh close to the foil, *edge sizing* was used around the edges. The *edge sizing* was given a bias, so that the elements were finer at the leading edge of the foil, which had a larger curvature. The mesh close to the surface of the foil is shown in Figure 10.7.

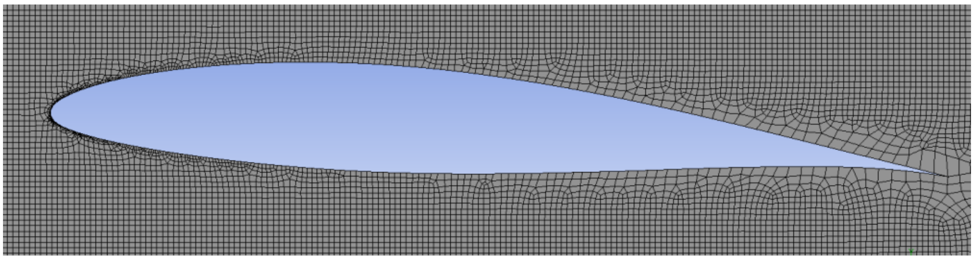

Figure 10.7 The mesh close to the foil.

To decide how fine the mesh needed to be, a quality control was performed. Different numbers of elements were tried for the geometry and test-simulations were run. The results of these simulations are shown in Table 10.4.

Table 10.4 Result of the quality control.

Mesh	***Number of elements***	***Cl***
1	51732	0.720
2	119195	0.742
3	256863	0.749

Despite using significantly more elements in Mesh 3 than Mesh 2, there was only a small impact of the result. The simulations were therefore believed to converge around this value. It was still desirable to have the simulations as accurate as possible, therefore Mesh 3 was chosen. However, increasing the amount of elements even further, would increase the simulation time significantly, which would be too impractical and time-consuming considering the amount of simulations that were needed.

The final settings for the mesh is presented below. The *faze sizing* is presented in Table 10.5, and the settings used for the edge sizing in Table 10.6.

Table 10.5 Settings for face sizing.

	Face sizing [m]
Rectangle A	0.1
Rectangle B	0.02
Rectangle C	0.0008

Table 10.6 Settings for edge sizing.

Number of divisions	250
Bias factor	50

10.4.3 **Boundary conditions**

The settings for the boundary conditions used in the simulations are presented below:

- The velocity magnitude at the inlet was set to 5.5 m/s, which roughly translates to 10 knots of boat speed.
- The pressure at the outlet was set to 0 Pa.
- The airfoil was set as a stationary wall with no slip.
- The upper surface was set as a stationary wall with specified shear to closer resemble the behavior of the water surface.
- The lower surface was set as a moving wall with no slip.

10.4.4 **Turbulence model**

The turbulence model used was the SST k-ω model, which is a combination of the k-ω model and the k-ε model. This model is known to perform well for low Reynolds numbers, which was suitable in this case [37].

10.4.5 **Results of the 2D CFD simulations**

In this section, the results from the 2D simulations in ANSYS are shown**.**

The static pressure around the airfoil with $\alpha = 0^o$ is shown in Figure 10.8. As described is section 2.1.5, there was an area of lower pressure on the upper surface of the airfoil, and a focused area of high pressure at the stagnation point at the leading edge.

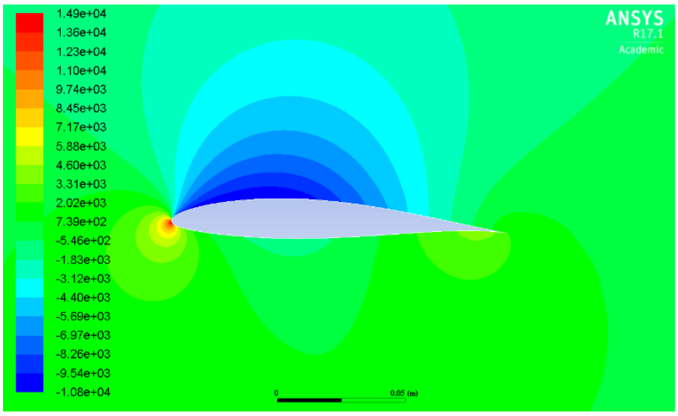

Figure 10.8 The static pressure around the foil.

The simulated *Cl*-values for the foil with and without flap are shown in Table 10.7 and 10.8 respectively. In table 10.7 different angles of attack for the entire airfoil were simulated. In table 10.8, the airfoil was kept at a zero-degree angle of attack, as different flap angles were simulated instead.

Table 10.7 Cl, no flap; varying α

α	*Cl*
-4	-0.109
-2	0.091
0	0.303
2	0.524
4	0.750
6	0.909
8	1.137
10	1.208
12	1.206

Table 10.8 Cl, with flap; α = 0; varying α_f

α_f	*Cl*
-4	0.018
-2	0.141
0	0.266
2	0.369
4	0.513
6	0.449
8	0.611
10	0.570
12	0.594
14	0.650
16	0.740

10.5 Comparison between XFOIL and ANSYS

The simulations of the NACA 63-412 airfoil without flap made in ANSYS provided values which were slightly lower than the corresponding values obtained by XFOIL. These values can be seen in Figure 10.9. It is however a well-known phenomenon that XFOIL overestimates the maximum *Cl* slightly [35]. Therefore, this data obtained from ANSYS was considered reliable.

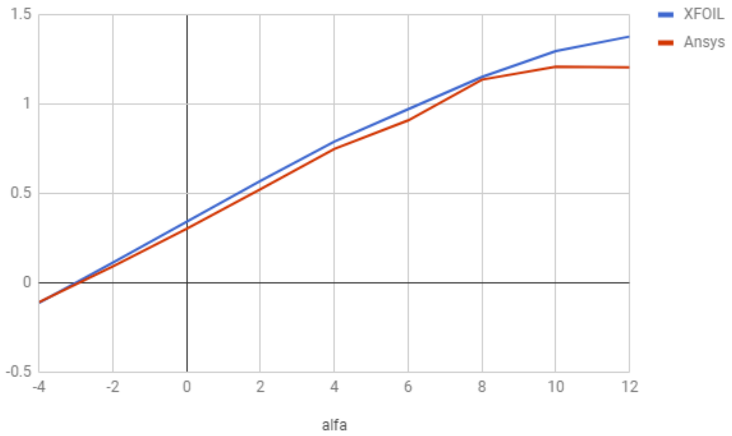

Figure 10.9 Comparison for Cl between XFOIL and ANSYS for a foil with no flap.

The data for the NACA 63-412 airfoil with flap turned out to be more difficult to simulate however. As can be seen in Figure 10.10, the simulations in ANSYS provided significantly lower values than the ones given by XFOIL. This deviation was greater than what could be expected from a slight overestimation by XFOIL. (The reason why the simulations for the flap did not turn out so well in ANSYS will be discussed more in depth in Chapter 14).

It was instead decided to use the *"rule of thumb"* described in section 2.1.7 to estimate the *Cl* for the airfoil with a flap, based on the *Cl* generated for a wing without a flap.

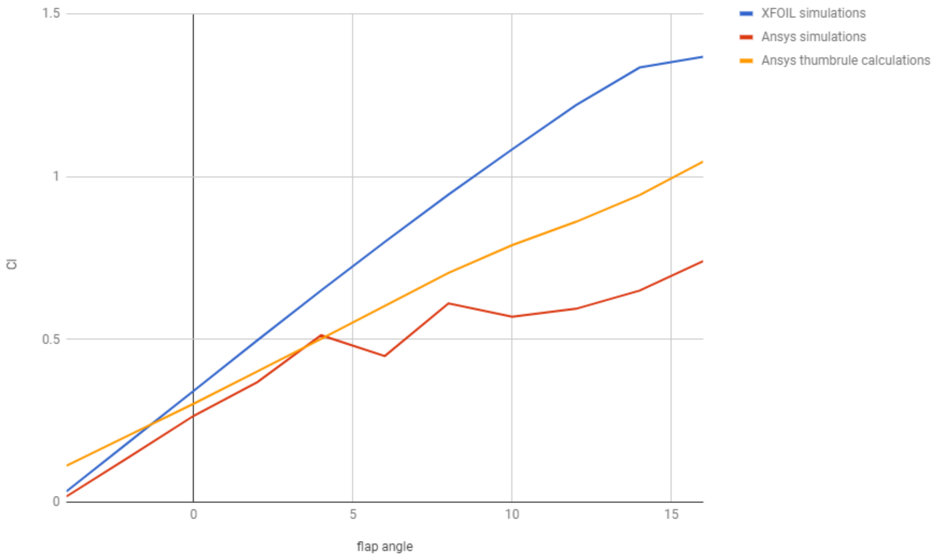

Figure 10.10 Comparison for Cl between XFOIL and ANSYS for a foil with a flap.

The *rule of thumb* was used to calculate the *Cl* for the flap as 45% of *Cl* for a wing without a flap. The results can be seen in Figure 10.10, and is somewhere between the *Cl* values given by XFOIL and ANSYS respectively. In the end, the data calculated with the *rule of thumb* based on the ANSYS simulations, was used for the calculations of the final area of the foils.

It was assumed that the maximum *Cl/Cd-ratio* would appear at the same angle of attack for the ANSYS simulations as for the XFOIL simulations.

The data that would be used in the calculations of the final areas is shown in the Table 10.9-10.10 below.

Table 10.9 Data for a foil with no flap.

Cl at $\boldsymbol{\alpha = 0^o}$	***Cl at max Cl/Cd*** $\boldsymbol{(\alpha = 4^o)}$
0.303	0.750

Table 10.10 Data for a foil with a flap.

Cl at $\boldsymbol{\alpha_f = 0^o}$	***Cl at max Cl/Cd*** $\boldsymbol{(\alpha_f = 13^o)}$
0.303	0.902

10.6 Designing the lifting foils

In this section, the steps leading to the final design of the lifting foils are explained.

10.6.1 Determining the lifting areas

Calculating the final areas of the centerboard and rudder foils was done by the following process:

1) The relevant data for Cl was obtained from ANSYS.
2) This data was used with Equation (10.10), (10.11) and (10.16), derived in section 10.2.3, to calculate the resulting areas and takeoff velocity for the foils.
3) Various angles of attack, velocities and areas were tested during these calculations, and by this iterative process, the final dimensions were set.

Apart from the data given in Table 10.9 and 10.10, the following input data, presented in Table 10.11, was used to calculate the lifting areas based on the "foiling at cruising speed" scenario:

Table 10.11 Input data for the final lifting area calculations.

L_c	70% of total lift
L_r	30% of total lift
Angle of attack centerboard	0 degrees
Angle of attack rudder	0 degrees
Crusing foiling speed	10.28 knots
Weight (boat+sailor)	140 kg

This input data resulted in an acceptable takeoff speed and an area that was considered reasonable compared to the lifting areas for the dinghies studied during the benchmarking. The final lifting areas and their corresponding takeoff speed are shown in Table 10.12.

Table 10.12 The final area for the foils.

Mean chord [mm]		***Area [m²]***		
Centerboard	***Rudder***	***Centerboard***	***Rudder***	***Takeoff speed [knot]***
219	135	0.3	0.12	6.67

10.6.2 **Planform**

With the areas decided for the lifting foils, the planforms could be designed.

The size of the flap of the centerboard foil was set to 30% of the chord, since all the foils studied during the benchmarking used this very configuration. The location of the hinge was therefore set to 30% chord from the trailing edge.

The hinge had to be a perfectly straight line to be able to rotate freely. To accommodate this, a sweep angle of 9.14º, and a dihedral angle of 1.6º was used.

Since the area and wingspan was set, the aspect ratio could be calculated using Equation 2.2. This resulted in an aspect ratio of $AR = 6.3$.

From Figure 2.3, the optimal taper ratio for the sweep angle of 9.14º was given as $TR = 0.35$.

The planform of the rudder foil was designed using the same principles as the centerboard foil. The wingspan and chord were chosen such that the aspect ratio of the rudder foil would match the aspect ratio of the centerboard foil. However, since the rudder foil had no flap, there were no restrictions of keeping a straight line for the 30% chord from the trailing edge. As can be seen in Figure 2.9, the optimal taper ratio is 0.45, to generate the lowest amount of drag. It was therefore decided to use this taper ratio for the rudder foil. In Figure 2.3, it can be seen that the optimal sweep angle for this taper ratio is zero degrees, which was used for the final design of the planform.

10.7 Designing the struts

As could be seen from the benchmarking in section 7.2.3, 400 mm was regarded as a normal submergence depth of the foils. An additional 500 mm was added since this was thought to allow sufficient clearance over most of the smaller waves. This meant that the depth of the centerboard was set to 900 mm.

Based on the benchmarking it was decided to use the same depth for the rudder and the centerboard. Consequently, the depth of the rudder was set to 900 mm to match the depth of the centerboard.

Since the new rudder was made a lot deeper than the original rudder for the Europe-dinghy, its area was increased. Therefore, the chord of the rudder-strut could be made a lot shorter. However, even though making the chord significantly shorter, the rudder area was still larger than the rudder of a standard Europe-dinghy. This meant that the resultant of the hydrodynamic force on the boat would be further back than normal, which would make the dinghy laterally imbalanced. To compensate for this, the centerboard had to be angled forward to redistribute the submerged area of the dinghy. This had another positive effect since a forward angled centerboard strut meant a larger distance between the centerboard foil and the rudder foil. The result of this was that the downwash from the centerboard foil would have less effect on the rudder foil.

One criteria was that it should be possible to change the angle of attack of the rudder manually (see Chapter 9). The solution to this was that the sailor loosens a bolt on the rudder head, angles the rudder to its desired position, and then tightens the bolt again. The friction between the rudder head and the rudder-strut would thus be used to keep the rudder fixed after the correct angle was chosen. This solution would also permit gradual deflection of the angle, which was favorable.

10.8 Designing the control system

As described in section 9.2, it was decided to use the concept *"wand integrated in the centerboard"*.

It was decided to use the simplest possible solution for the control system. All dinghies studied during the benchmarking used fully mechanical automatic control systems of different kinds. A similar mechanical system was therefore developed for this project.

It was reasonable to believe that small inaccuracies between the final prototype and the drawings would occur. Therefore, it would be beneficial to have an interface where the settings of the control system easily could be fine-tuned on the prototype. Being able to change the deflection of the flap for a given change of angle of the wand, referred to as *gearing*, was crucial. It was also desirable to have the ability of changing the ride height during stable foiling, at will. The interface would need to incorporate this function as well.

10.9 Description of the final design

In this section, the final design of the prototype will be shown and explained.

10.9.1 **The lifting foils**

As previously stated, the aim was to design hydrofoils that could takeoff already at low speeds. This was considered while doing the area-calculations. Consequently, the resulting foils had large areas compared to the foils used by the dinghies studied during the benchmarking. One tradeoff was therefore that these larger foils would generate more drag, which would prevent high top speeds. However, this was not an important factor according to the product specifications. The final areas for the foils were:

- Area for the centerboard foil: 0.3 m^2
- Area for the rudder foil: 0.12 m^2

The final planforms for the centerboard and rudder foil are presented in Figure 10.11 and Figure 10.12 respectively. The leading edges are facing to the left. (Note that the foils are designed with a hole in the center to provide for easier assembly with the struts during construction).

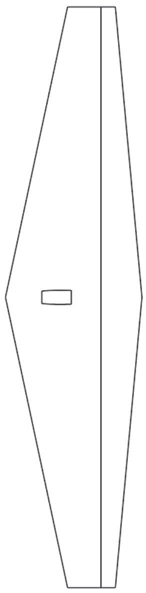

Figure 10.11 Planform of the centerboard foil.

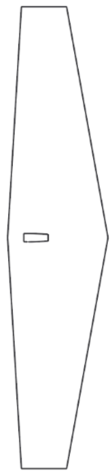

Figure 10.12 Planform of the rudder foil.

10.9.2 **The struts**

It was decided that the centerboard and the rudder both should have a depth of 900 mm. The planforms for these are seen in Figure 10.13 and 10.14 below. The bottom parts of the struts are shaped for an easy fit to the corresponding holes in the foils.

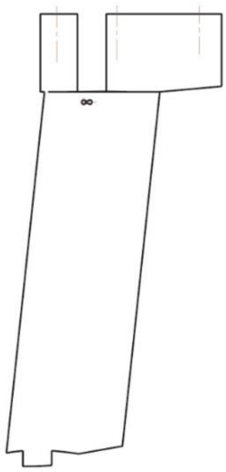

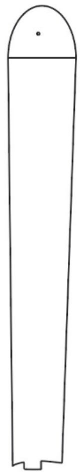

Figure 10.13 Planform for the centerboard strut. **10.14 Planform for the rudder strut.**

10.9.3 The control system

Based on the reasoning in section 10.8, a design for the control system was developed. In Figure 10.15 below, a thorough sketch of the control system is shown.

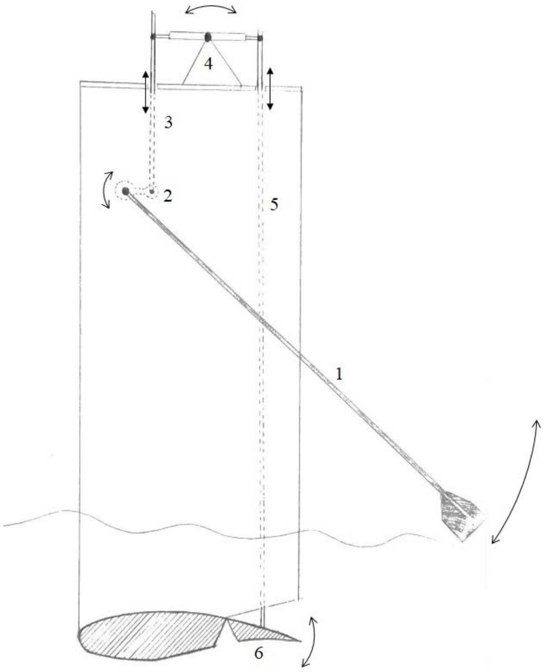

Figure 10.15 A sketch explaining the control system.

The *wand* (1) is dragged along the surface of the water. When the ride height of the dinghy is changed, the angle of the wand is changed. The wand is connected to the *lever* (2) inside of the centerboard, which in turn rotates and affects the *vertical link* (3) with motion directed either upwards or downwards. This movement is redirected through the *seesaw* (4), affecting the *pushrod* (5) with motion in the opposite direction. The pushrod is connected to the top surface of the *flap* (6) and can thereby change the angle of the flap.

The *seesaw* was made by a turnbuckle, welded on a small Ø8 mm stainless steel rod, allowing it to rotate freely in the central plane of the centerboard. The leverage of the arms of the seesaw can be modified, thus allowing the gearing of the system to be changed. The point of contact between the *seesaw* and the *vertical link* can also be changed, to set the ride height during stable foiling.

The *plate* that the interface (seesaw) was connected to was also designed to enable clamping of the centerboard. Clamping of the centerboard was necessary to keep it oriented correctly and to not fall off when sailing in displacement mode.

Both the *plate* and *lever* were 3D printed. CAD models of these parts can be seen in Figure 10.16-10.17 below.

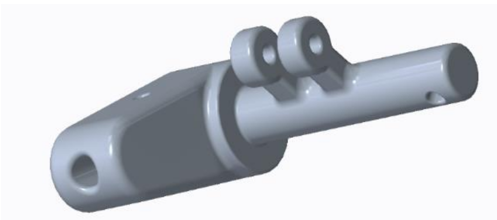

Figure 10.16 3D model of the lever.

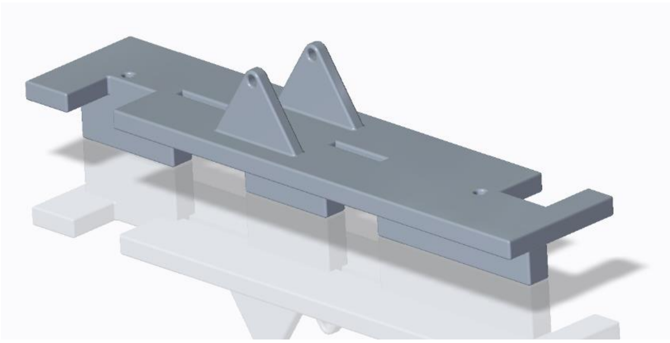

Figure 10.17 3D model of the plate.

11 Building the prototype

In this chapter, the building of the prototype is described.

11.1 Material

The foils have thin profiles, but still need to have sufficient strength. It was also of importance to keep the foils as lightweight as possible to favor foiling. Therefore, they were built out of carbon fiber, using epoxy as resin. Most foils today are built using these materials, which means that it is a well-tested and proven method.

11.2 Building method

The foils were built using female molds, which means that the material is applied inside a mold, and that the layer of carbon fiber closest to the mold will become the outer surface of the finished wing. An alternative would be to use the mold as a core and apply carbon fiber to the outside, referred to as a male mold. However, the advantage of using a female mold is that the surface finish of the carbon fiber will be better straight out of the mold. This means that less post-processing with filler and grinding will be needed, which saves weight [38]. The foils were made in two halves and later glued together.

11.3 The building process

The building process consisted of the steps listed below. The entire process is described in detail in Appendix E.

1. *Designing the molds*
   CAD models of the female molds were created in Creo Parametric.
2. *Building the molds*
   CNC milling was used to manufacture the molds. Poplar was used as material.

3. *Arrangement of carbon fiber*
   Carbon fiber was arranged in the molds to withstand the forces that would arise during foiling as efficiently as possible.
4. *The vacuum infusion process*
   The carbon fiber was injected with epoxy using vacuum infusion.
5. *Constructing the hinge*
   The hinge between the centerboard foil and the flap was constructed out of a strip of fiberglass.
6. *Post-processing the wing halves*
   The wing halves were cut and grinded to their intended shape. Thereafter the halves were fitted with reinforcements.
7. *Gluing the wing halves together*
   The halves were joined together using composite glue.
8. *Creating the centerboard plateau*
   A plateau where the hull would rest during foiling was created around the centerboard strut, by applying carbon fiber directly to the hull to ensure a perfect fit. Release tape was used to avoid the carbon fiber sticking to the hull.
9. *Connecting the struts to the foils*
   The struts were glued to the foils using composite glue.
10. *Building the control system*
    The various parts used in the control system were crafted in a metal workshop. The *plate* and the *lever*, were 3D printed due to their complex geometry.
11. *Fitting the hydrofoils to the hull*
    Due to the plateau, the centerboard had to be inserted from underneath the boat. It was thereafter locked into position on the *plate* by tightening three wingnuts on threaded rods connected to the centerboard. The original rudder head was modified and fitted to the hull as it was originally intended to.

12 Testing

To be able to draw conclusions regarding whether the prototype worked or not, a test was carried out at sea.

The test was carried out at the sea outside Limhamns småbåtshamn in Malmö, December 21, 2017. The wind strength was 10-14 knots with fairly choppy sea.

A rib boat was borrowed by Malmö Seglarsällskap. This was partly due to security, considering the near freezing water temperatures, and partly due to that it was the first time the hydrofoils were tested. The rib boat also made it possible for the crew to document the tests with video cameras.

The focus of this test was to check all the systems to make sure that they worked properly. No additional instruments were used to measure the performance of the dinghy.

The test piloting was done by the authors themselves. Although having sailed for their entire lives, it should be noted that neither of the authors had any previous practical experience from sailing a foiling boat.

13 Results

In this chapter, the results of the project are presented. The final design, pictures of the finished prototype and the results from the test are shown.

13.1 The final design

Renderings of the final design of the hydrofoils are shown in Figure 13.1-13.2.

Figure 13.1 Rendering of the final design.

Figure 13.2 Rendering of the final design.

Simplified drawings of the final design are presented in Appendix F.

13.2 The prototype

Pictures of the prototype can be seen in Figure 13.3-13.5.

Figure 13.3 The centerboard.

Figure 13.4 The rudder.

Figure 13.5 The centerboard and rudder fitted to the hull of the Europe-dinghy.

13.3 Test results

During the test, the dinghy was able to foil for shorter periods of time. This can be seen in Figure 13.6.

Figure 13.6 Successful foiling.

The centerboard foil was clearly producing enough lift to encourage foiling in these conditions. However, after testing the hydrofoils for a while, it was noted that the stern started to stick to the surface of the water, even though the centerboard foil generated enough lift to initiate foiling. This tendency can be seen in Figure 13.7. As it turned out, the solution of keeping the rudder angle fixed using only friction was not enough, and the rudder was slowly pushed backwards during foiling. This meant the angle of attack of the rudder eventually became too low, which explains why not enough lift was created by the rudder foil.

Figure 13.7 The centerboard foil creates enough lift to foil, but the rudder foil does not.

The control system worked as intended during the periods of successful foiling.

14 Discussion

In this chapter, aspects that could have affected the outcome of the results are discussed.

14.1 General discussion

A design has been developed and a prototype has been built and tested successfully. The information obtained from this process answered the research questions that were defined in the introduction of the report. Thus, the goal of this thesis work has been achieved.

The simulations in ANSYS did not provide satisfactory results when simulating foils with a flap. It is unclear why this was the case, especially when bearing in mind that the ANSYS simulations of the foils without flaps provided credible results. One explanation might be found in the setup of the geometry of the foils with flaps. It was not possible to generate a mesh with a flap attached directly to the upper surface of the foil. Therefore, in practice, a minuscule gap had to be introduced between the flap and the foil. This gap might be part of the explanation of the unsatisfactory results.

It is also conceivable that better simulation results could have been obtained if additional turbulence models were tried. However, due to the strict time limit of this project, only the trusted and commonly used SST k-ω model was used.

It would have been preferable to run 3D simulations in CFD to study the effect of the water surface on the foils, and the interaction between the two foils, such as the downwash from the centerboard foil affecting the rudder foil. Due to the problems of getting accurate results from the 2D simulations of the foil with a flap, there was no time left to carry out any 3D simulations. It was prioritized that the build should start on time, instead of being postponed due to further simulations, thus running the risk of not having the prototype finished on time. Data that could be gathered when building and testing the prototype, was considered more useful for the purpose of this thesis, than running additional simulations. It is however likely that a more optimized design could be developed using CFD simulations in 3D.

The general idea that lead to this project was to develop a more cost-efficient way to experience hydrofoiling than the alternatives that were already on the market.

However, during the scope of this project only one prototype was to be made, to be used as a proof of concept. To be able to evaluate the concept in the most efficient way possible, it was undesirable to have the foils break due to material failure originating from the use of too weak materials. This could have made it complicated to assess whether the entire concept was plausible or not. Since the maximum forces that would act on the foils were unknown, carbon fiber – a well-tested, strong, light weight and expensive material – was used. In a future potential product, the choice of materials would of course have to be optimized for low cost.

The extent of this project rendered it inconceivable to delve into too much detail associated with each separate aspect of the project. To optimize the results further, additional work would be needed.

The testing of the hydrofoils at sea outside of Malmö was carried out in marginal wind conditions. Despite of this, the Europe-dinghy was able to foil for shorter periods of time, which was considered a big success. The test showed that the centerboard foil generated enough lift. However, the rudder foil did not. As stated before, keeping the rudder angle fixed using only friction was not sufficient. Therefore the rudder angle slowly decreased during foiling. Significantly improved results would most likely be obtained by fixing the rudder angle.

A test during stronger winds would mean that the Europe-dinghy could reach even higher speeds in displacement mode, which would also favor foiling. However, there was unfortunately not enough time for a second attempt during the extent of this project.

It should also be noted that neither of the two sailors (the authors of this thesis) had ever sailed a foiling boat before. Sailing this kind of boat is different compared to sailing ordinary dinghies. It requires a special, fine-tuned, technique and is thus rather difficult to learn. Consequently, this was a challenge. A sailor with greater foiling experience would therefore likely be able to foil during longer periods of time already during the first test.

14.2 Sources of error

Factors that might have affected the outcome of the results are presented below.

- No 3D analysis was carried out. This meant that the effects the centerboard foil had on the rudder foil was unknown.
- No Velocity Prediction Program (VPP) was used. By using one, the theoretical velocities during foiling could have been calculated, and the lifting areas could have been determined in a more precise manner.
- The foils were not built by professionals. This meant that a few imperfections in the final physical prototype arose. For instance, when processing the wing-halves by cutting and grinding the edges to their

intended size, one millimeter too much or too little would affect the entire shape of the wing when the halves were glued together.

15 Conclusions

In this chapter, the conclusions drawn from this thesis work are described. An outlook with suggestions for potential future work of this project is also presented.

15.1 General conclusions

As stated in the introductory chapter of this report, the aim of the project was to investigate if a Europe-dinghy could be complemented with separate hydrofoils in a simple and practical manner. A prototype was therefore built and tested, as a proof of concept.

This project has shown that it is possible to fit separate hydrofoils to a Europe-dinghy in a practical manner.

It has also shown that a Europe-dinghy can be fitted with a new centerboard and rudder equipped with hydrofoils, without making any permanent changes to the hull. The new centerboard and rudder are easily attached and detached (in about 10 minutes time of mounting with no special tools). The solution of having the hull resting on a plateau on the centerboard strut, while clamping the strut against the top of the centerboard case works well. However, the way the angle of the rudder was fixed, by just clamping it in the rudder head, is not sufficient.

The initial test has shown that the Europe-dinghy is in fact able to hydrofoil, using these detachable hydrofoils, for shorter periods of time. The centerboard foil easily generates enough lift to initiate foiling. However, the test has also shown that, during foiling, the rudder is slowly angled backwards and eventually obtains too low an angle of attack, and, consequently, cannot generate the intended amount of lift.

The initial test has also proved that the hull of a Europe-dinghy is able to withstand the forces during foiling, without any reinforcements. However, more testing is required to draw a definite conclusion.

An active, fully mechanical, control system was developed to control the amount of lift generated, and thereby provide stable foiling. The test has shown that the system works as intended but may be further refined given more time.

15.2 Suggestions for further testing and development

Suggestions for future work and a possible proceeding to a real product are presented below.

- Further testing is needed to make sure that the hull can withstand the forces during foiling. The boat should be tested in more extreme weather conditions. It should also be tested for extended periods of time, to make sure that material fatigue is not a factor. Sailors of different weights should also test the boat to study the effects this has on the performance of the hydrofoils.
- The product specifications would have to be weighted in a different manner for a real product. More bias should be applied to the user friendly-aspects, such as easy transportation, easy launch and easy assembly. Based on the knowledge gathered during this project, new, better concepts, focused on fulfilling the newly weighted product specifications, should be generated.

  One simple way of making the product more user friendly would be to make the foils detachable from the struts using screw joints. This would facilitate transport and storage of the foils.

  It could also be beneficial to develop a system that allows the centerboard to be retracted directly into the hull, after it has been inserted from underneath. This would make it possible to singlehandedly launch the dinghy from a trolley, instead of asking four friends to help carry the dinghy in an inclined fashion (to avoid damaging the hydrofoils) into the water.

- A new system of keeping the rudder angle fixed in the rudder head is needed. This can easily be done by drilling a series of holes through the rudder head and using sprints to set the desired angle of the rudder.

  In this project, the rudder head of the original Europe-dinghy was repurposed and used to attach the new hydrofoil-equipped rudder. However, the best thing would probably be to not modify an existing rudder head, but instead have a completely new one purpose built. In this way, a more sophisticated solution for changing the rudder angle could be developed.
- A cover should be used for the interface for the control system, both to protect the interface from being damaged, and to make sure that the sailor is not hurt on it during a crash.

16 References

[1] Neilson Bonikowsky, L. (2009, March 25). Hydrofoil. Retrieved January 1, 2018, from http://www.thecanadianencyclopedia.com/en/article/hydrofoil/

[2] Government of Canada. (2012). Bell HD-4. Retrieved January 2, 2018, from https://commons.wikimedia.org/wiki/File:Bell_HD-4.jpg

[3] Watters, S. (2017). America’s Cup. Retrieved January 3, 2018, from https://nzhistory.govt.nz/culture/americas-cup

[4] Wikimedia Commons. (2017). 2013 America's Cup, race 1, mark 1. Retrieved December 28, 2017, from https://commons.wikimedia.org/wiki/File:2013_America%27s_Cup,_race_1,_mark_1.JPG

[5] International Europe Class. (2013). Retrieved January 3, 2018, from http://www.europeclass.org/introduction.html

[6] Essiq AB. (2018). Retrieved January 7, 2018 from http://www.essiq.se/om-oss/

[7] Anderson, J. D, JR. (2011). Fundamentals of Aerodynamics, Fifth Edition in SI Units. New York: McGraw-Hill Education.

[8] Larsson, L., Eliasson R. E., Orych M. (2014). Principles of Yacht Design, Fourth Edition. Camden, Maine: International Marine/McGraw-Hill Education.

[9] NASA Glenn Research Center. (2015). Wing Geometry Definitions. Retrieved December 27, 2017, from https://www.grc.nasa.gov/www/k-12/airplane/geom.html

[10] NASA Glenn Research Center. (2015). What is Lift?. Retrieved December 27, 2017, from https://www.grc.nasa.gov/www/k-12/airplane/lift1.html

[11] NASA Glenn Research Center. (2015). What is Drag?. Retrieved December 27, 2017, from https://www.grc.nasa.gov/www/k-12/airplane/drag1.html

[12] Coanda Effect. (2014). Retrieved December 27, 2017, from http://www.thermofluids.co.uk/effect.php

[13] NASA Glenn Research Center. (2015). Bernoulli and Newton. Retrieved December 27, 2017, from https://www.grc.nasa.gov/www/k-12/airplane/bernnew.html

[14] NASA Glenn Research Center. (2015). Inclination Effects on Lift. Retrieved December 27, 2017, from https://www.grc.nasa.gov/www/k-12/airplane/incline.html

[15] NASA Glenn Research Center. (2015). Downwash Effects on Lift. Retrieved December 27, 2017, from https://www.grc.nasa.gov/www/k-12/airplane/downwash.html

[16] NASA Glenn Research Center. (2015). Factors that Affect Lift. Retrieved December 27, 2017, from https://www.grc.nasa.gov/www/k-12/airplane/factors.html

[17] NASA Glenn Research Center. (2015). Shape Effects on Lift. Retrieved December 27, 2017, from https://www.grc.nasa.gov/www/k-12/airplane/shape.html

[18] NASA Glenn Research Center. (2015). Lift to Drag Ratio, L/D Ratio. Retrieved December 27, 2017, from https://www.grc.nasa.gov/www/k-12/airplane/ldrat.html

[19] NASA Glenn Research Center. (2015). Flaps and Slats. Retrieved December 27, 2017, from https://www.grc.nasa.gov/www/k-12/airplane/flap.html

[20] Beaver, B., Zseleczky, J. (2009). Full Scale Measurements on a Hydrofoil International Moth. Annapolis, Maryland: The 19th Chesapeake Sailing Yacht Symposium.

[21] Andersson, A., Barreng, A., Bohnsack, E., Larsson, L., Lundin, L., Sahlberg, R., et al. (2017). The Foiling Optimist. Lorient, France: The Fourth International Conference on Innovation in High Performance Sailing Yachts.

[22] Andrew McDougall launches the all new WASZP Moth. (2015). Retrieved December 28, 2017, from http://www.sailweb.co.uk/dinghy/25216/andrew-mcdougall-launches-the-all-new-waszp-moth

[23] May, A. (2005). The Foiling Guide. Retrieved October 15, 2017, from http://www.mothclass.at/wp-content/uploads/2014/10/Foiling-Guide.pdf

[24] Faltinsen, O. M. (2005). Hydrodynamics of High-Speed Marine Vehicles. New York: Cambridge University Press.

[25] Ulrich, K. T., Eppinger, S. D. (2012). Product Design and Development (5th ed.). London, United Kingdom: McGraw-Hill.

[26] Wiberg, O., Mechanical Engineer, Corebon AB, Malmö, Sweden. Personal conversations (2017).

[27] IMCA UK. (2016). Retrieved September 10, 2017, from http://www.internationalmoth.co.uk/the-moth/history/

[28] Learn More About the Waszp. (2018). Retrieved September 10, 2017, from http://www.waszp.com/

[29] Glide Free Foils. (2017). Retrieved September 10, 2017, from http://www.glidefree.com.au/Media.html

[30] Airfoil Tools. (2017). Retrieved October 2, 2017, from www.airfoiltools.com

[31] Barden, T. A., Binns, J. R. (2012). On the Road to Establishing Ventilation Probability for Moth Sailing Dinghies. Launceston, Australia: 18th Australasian Fluid Mechanics Conference

[32] Jardine, M. (May 29, 2017). [Image of Moth dinghy]. Retrieved January 3, 2018, from https://www.flickr.com/photos/134386166@N03/34937555686/in/album-72157684334871896/

[33] Wikimedia Commons. (January 1, 2014). [Image of Glide Free Foils on Laser]. Retrieved December 28, 2017, from https://commons.wikimedia.org/wiki/File:Glide_Free_Foils_on_Laser.jpg

[34] Drela, M. (2008). XFOIL. Retrieved October 15, 2017, from http://web.mit.edu/drela/Public/web/xfoil/

[35] Aerofoil Engineering. (n.d.). Retrieved October 15, 2017, from http://aerofoilengineering.com/Validation.php

[36] The Engineering Toolbox, Water - Density, Specific Weight and Thermal Expantion Coefficient. (n.d.). Retrieved October 15, 2017, from https://www.engineeringtoolbox.com/water-density-specific-weight-d_595.html

[37] SST k-omega Model. (2011). Retrieved October 20, 2017, from https://www.cfd-online.com/Wiki/SST_k-omega_model

[38] Mold Construction. (n.d.). Retrieved January 5, 2018, from http://www.fibreglast.com/product/mold-construction/Learning_Center

Appendix A Price comparison

In this Appendix, typical prices for purpose-built hydrofoiling dinghies are compared to typical prices for a Europe-dinghy. This way, the magnitude of the difference in price is illustrated.

The price of brand new sailing dinghies vary significantly depending on the complementary equipment. It is therefore difficult to make comparisons of their respective prices. Since the idea behind this project was to develop a budget alternative for a foiling dinghy, the secondhand market of dinghies were studied instead. This was thought to be more relevant for a sailor wanting a budget alternative.

In Tables A.1-A.3 below, second hand prices for purpose-built foiling Moth- and Waszp-dinghies, and regular Europe-dinghies are compiled. The prices presented in the tables are based on several adverts posted on buy/sell-websites for used dinghies. This provides an overview of typical differences in price for these dinghies.

Table A.1 Second hand prices for a Moth [A1].

Highest price	399,000 SEK
Average price	190,000 SEK
Lowest price	90,000 SEK

Table A.2 Second hand prices for a Waszp [A2].

Highest price	150,000 SEK
Average price	110,000 SEK
Lowest price	90,000 SEK

Table A.3 Second hand prices for a Europe-dinghy [A3].

Highest price	63,500 SEK
Average price	25,000 SEK
Lowest price	9,000 SEK

References Appendix A

[A1] Mothmart.com - World International Moth Marketplace. (n.d.). [Online marketplace for buying and selling Moth dinghies]. Retrieved September 20, 2017, from http://www.mothmart.com/category/foiling-moth/

[A2] Mothmart.com - World International Moth Marketplace. (n.d.). [Online marketplace for buying and selling Moth dinghies]. Retrieved September 20, 2017, from http://www.mothmart.com/tag/waszp/

[A3] Jolleplan. (n.d.). [Online marketplace for buying and selling sailing dinghies]. Retrieved September 20, 2017, from http://jolleplan.se/category/e-jolle/

Appendix B Product specifications

In the tables below, the full lists of criteria for the three sub-concepts that were defined in Chapter 5, are presented.

The criteria are weighted on a scale from 1-5, 1 being the least and 5 being the most important. The product specifications for the centerboard, rudder and control system are presented in Table B.1-B.3 below.

Table B.1 Product specifications for the centerboard.

Centerboard		
Specifications	**Weight**	**%**
Function		
Foiling at low speeds	5	7,94%
Reaching high speeds	2	3,17%
Stable foiling	5	7,94%
Good sailing characteristics in displacement mode	3	4,76%
Automatic control of angle of attack	5	7,94%
Durable	4	6,35%
For the user		
User friendly	1	1,59%
No permanent changes of the dinghy	5	7,94%
Esthetic	1	1,59%
Easy to install	1	1,59%
Ability to adjust settings	5	7,94%
Long lifespan	1	1,59%
Low cost	2	3,17%
Easy to launch	1	1,59%
Easy to transport	1	1,59%
Easy to store	1	1,59%
Production		
Easy to manufacture	4	6,35%
Few moving parts	4	6,35%
Low technical complexity	4	6,35%
Safety		
The sailor is not hurt more than necessary	3	4,76%
The hydrofoils can cope with the forces involved	5	7,94%
Sum	63	100,00%

Table B.2 Product specifications for the rudder.

Rudder		
Specifications	**Weight**	**%**
Function		
Foiling at low speeds	5	8,33%
Reaching high speeds	2	3,33%
Stable foiling	5	8,33%
Good sailing characteristics in displacement mode	3	5,00%
Automatic control of angle of attack	1	1,67%
Durable	4	6,67%
For the user		
User friendly	1	1,67%
No permanent changes of the dinghy	5	8,33%
Esthetic	1	1,67%
Easy to install	1	1,67%
Ability to adjust settings	5	8,33%
Long lifespan	1	1,67%
Low cost	2	3,33%
Easy to launch	1	1,67%
Easy to transport	1	1,67%
Easy to store	1	1,67%
Production		
Easy to manufacture	4	6,67%
Few moving parts	4	6,67%
Low technical complexity	5	8,33%
Safety		
The sailor is not hurt more than necessary	3	5,00%
The hydrofoils can cope with the forces involved	5	8,33%
Sum	60	100,00%

Table B.3 Product specifications for the control system.

Control System		
Specifications	**Weight**	**%**
Function		
Flap gearing adjustment	5	7,81%
Ride height adjustment	5	7,81%
Stable foiling	5	7,81%
Automatic control of angle of attack	5	7,81%
Durable	4	6,25%
For the user		
User friendly	4	6,25%
No permanent changes to the dinghy	5	7,81%
Esthetic interface	1	1,56%
Easy to install	2	3,13%
Ability to adjust settings	5	7,81%
Long lifespan	1	1,56%
Low cost	2	3,13%
Production		
Easy to manufacture	4	6,25%
Few moving parts	4	6,25%
Low technical complexity	4	6,25%
Safety		
The sailor is not hurt more than necessary	3	4,69%
The control system can cope with the forces involved	5	7,81%
Sum	64	100,00%

Appendix C Basic strength analysis for the static foiling case

In this Appendix, the calculations leading to the conclusion drawn in Chapter 6 is presented.

The forces involved when righting a capsized Europe-dinghy are shown in Figure C.1.

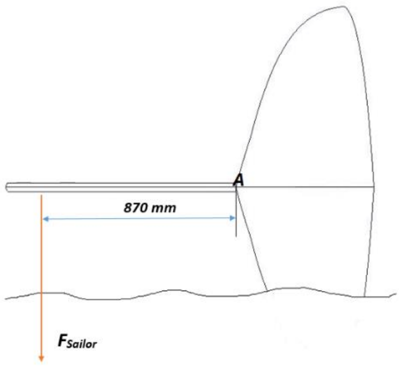

Figure C.1 The forces acting on a capsized dinghy during righting.

If the weight of the sailor is 85 kilograms, the moment acting on point A will be:

$$M_A = F_{sailor} * 0.87 = 85 * 9.82 * 0.87 = \mathbf{726.189\ Nm} \quad \text{(C.1)}$$

The forces acting on the dinghy while foiling are shown in Figure C.2.

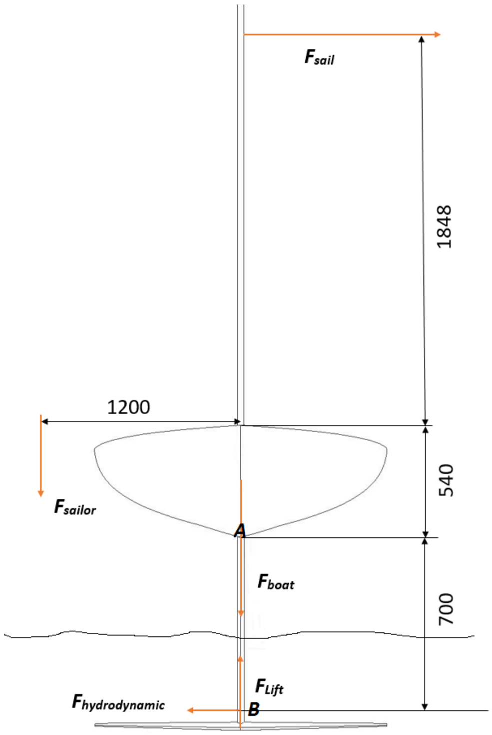

Figure C.2 The forces on a foiling dinghy.

Equilibrium around point B gives the following expression:

$$F_{sail} * (1.848 + 0.540 + 0.7) - F_{sailor} * 1.2 = 0 \quad \text{(C.2)}$$

$$\Leftrightarrow F_{sail} = \frac{F_{sailor} * 1.2}{1.848 + 0.540 + 0.7} = \frac{85 * 9.82 * 1.2}{3.088} = 304.635\ N \quad \text{(C.3)}$$

When F_{sail} is known, the moment around the point A can be calculated.

$$M_A = F_{sailor} * 1.2 - F_{sail} * (1.848 + 0.54) =$$

$$85 * 9.82 * 1.2 - 304.635 * 2.388 = \mathbf{274.172\ Nm} \quad \text{(C.4)}$$

Appendix D Concept selection matrices

In this Appendix, the concept selection matrices used to select the final concepts are shown.

The concept selection matrices for the centerboard, rudder and control system are shown in Table D.1-D.3.

Table D.1 The concept selection matrix for the centerboard.

Centerboard			Concepts							
			Angle the entire foil		Angle the entire centerboard		Flap with mechanical hinge		Flap with fiberglass hinge	
Specifications	**Weight**	**%**	*Score*	*Weighted score*	*Score*	*Weighted score*	*Score*	*Weighted score*	*Score*	*Weighted score*
Function										
Foiling at low speeds	5	7,94%	4	0,32	4	0,32	4	0,32	5	0,40
Reaching high speeds	2	3,17%	2	0,06	2	0,06	2	0,06	2	0,06
Stable foiling	5	7,94%	5	0,40	5	0,40	5	0,40	5	0,40
Good sailing characteristics in displacement mode	3	4,76%	5	0,24	3	0,14	5	0,24	5	0,24
Automatic control of angle of attack	5	7,94%	5	0,40	1	0,08	5	0,40	5	0,40
Durable	4	6,35%	2	0,13	4	0,25	4	0,25	5	0,32
For the user										
User friendly	1	1,59%	3	0,05	3	0,05	3	0,05	3	0,05
No permanent changes of the dinghy	5	7,94%	3	0,24	3	0,24	3	0,24	3	0,24
Esthetic	1	1,59%	3	0,05	3	0,05	3	0,05	3	0,05
Easy to install	1	1,59%	3	0,05	3	0,05	3	0,05	3	0,05
Ability to adjust settings	5	7,94%	5	0,40	3	0,24	5	0,40	5	0,40
Long lifespan	1	1,59%	3	0,05	3	0,05	3	0,05	3	0,05
Low cost	2	3,17%	3	0,10	3	0,10	3	0,10	3	0,10
Easy to launch	1	1,59%	3	0,05	3	0,05	3	0,05	3	0,05
Easy to transport	1	1,59%	3	0,05	3	0,05	3	0,05	3	0,05
Easy to store	1	1,59%	3	0,05	3	0,05	3	0,05	3	0,05
Production										
Easy to manufacture	4	6,35%	3	0,19	2	0,13	3	0,19	4	0,25
Few moving parts	4	6,35%	3	0,19	3	0,19	3	0,19	3	0,19
Low technical complexity	4	6,35%	3	0,19	2	0,13	3	0,19	4	0,25
Safety										
The sailor is not hurt more than necessary	3	4,76%	3	0,14	3	0,14	3	0,14	3	0,14
The hydrofoils can cope with the forces involved	5	7,94%	3	0,24	3	0,24	3	0,24	3	0,24
Sum	63	100,00%		3,56		2,98		3,68		**3,95**

Table D.2 The concept selection matrix for the rudder.

Rudder			Concepts							
			Angle the entire foil		Angle the entire rudder manually		Flap with mechanical hinge		Flap with fiberglass hinge	
Specifications	**Weight**	**%**	*Score*	*Weighted score*	*Score*	*Weighted score*	*Score*	*Weighted score*	*Score*	*Weighted score*
Function										
Foiling at low speeds	5	8,33%	5	0,42	5	0,42	5	0,42	5	0,42
Reaching high speeds	2	3,33%	2	0,07	2	0,07	2	0,07	2	0,07
Stable foiling	5	8,33%	5	0,42	5	0,42	5	0,42	5	0,42
Good sailing characteristics in displacement mode	3	5,00%	5	0,25	3	0,15	5	0,25	5	0,25
Automatic control of angle of attack	1	1,67%	5	0,08	1	0,02	5	0,08	5	0,08
Durable	4	6,67%	2	0,13	5	0,33	4	0,27	5	0,33
For the user										
User friendly	1	1,67%	3	0,05	3	0,05	3	0,05	3	0,05
No permanent changes of the dinghy	5	8,33%	3	0,25	3	0,25	3	0,25	3	0,25
Esthetic	1	1,67%	3	0,05	3	0,05	3	0,05	3	0,05
Easy to install	1	1,67%	5	0,08	5	0,08	5	0,08	5	0,08
Ability to adjust settings	5	8,33%	5	0,42	5	0,42	5	0,42	5	0,42
Long lifespan	1	1,67%	3	0,05	3	0,05	3	0,05	3	0,05
Low cost	2	3,33%	3	0,10	3	0,10	3	0,10	3	0,10
Easy to launch	1	1,67%	3	0,05	3	0,05	3	0,05	3	0,05
Easy to transport	1	1,67%	3	0,05	3	0,05	3	0,05	3	0,05
Easy to store	1	1,67%	3	0,05	3	0,05	3	0,05	3	0,05
Production										
Easy to manufacture	4	6,67%	3	0,20	3	0,20	3	0,20	3	0,20
Few moving parts	4	6,67%	3	0,20	5	0,33	3	0,20	3	0,20
Low technical complexity	5	8,33%	2	0,17	4	0,33	2	0,17	2	0,17
Safety										
The sailor is not hurt more than necessary	3	5,00%	3	0,15	3	0,15	3	0,15	3	0,15
The hydrofoils can cope with the forces involved	5	8,33%	3	0,25	3	0,25	3	0,25	3	0,25
Sum	60	100,00%		3,48		3,82		3,62		**3,68**

Table D.3 The concept selection matrix for the control system.

Control System			Concepts			
			Wand integrated in the centerboard		Wand hanging from the bow	
Specifications	**Weight**	**%**	*Score*	*Weighted score*	*Score*	*Weighted score*
Function						
Flap gearing adjustment	5	7,81%	5	0,39	5	0,39
Ride height adjustment	5	7,81%	5	0,39	5	0,39
Stable foiling	5	7,81%	2	0,16	5	0,39
Automatic control of angle of attack	5	7,81%	3	0,23	3	0,23
Durable	4	6,25%	4	0,25	2	0,13
For the user						
User friendly	4	6,25%	3	0,19	3	0,19
No permanent changes to the dinghy	5	7,81%	5	0,39	5	0,39
Esthetic interface	1	1,56%	4	0,06	2	0,03
Easy to install	2	3,13%	5	0,16	1	0,03
Ability to adjust settings	5	7,81%	4	0,31	4	0,31
Long lifespan	1	1,56%	3	0,05	3	0,05
Low cost	2	3,13%	3	0,09	3	0,09
Production						
Easy to manufacture	4	6,25%	3	0,19	2	0,13
Few moving parts	4	6,25%	3	0,19	2	0,13
Low technical complexity	4	6,25%	3	0,19	2	0,13
Safety						
The sailor is not hurt more than necessary	3	4,69%	3	0,14	3	0,14
The control system can cope with the forces involved	5	7,81%	3	0,23	3	0,23
Sum	64	100,00%		3,61		3,38

Appendix E The building process

In this Appendix, the process of building the prototype is described in chronological order.

E.1 Designing the molds

To create the molds, 3D models of these had to be made. The molds were simply made as negatives from the existing 3D models of the foils, and then split in to two halves. The CAD model of the mold for the upper surface of the centerboard foil is shown in Figure E.1 below.

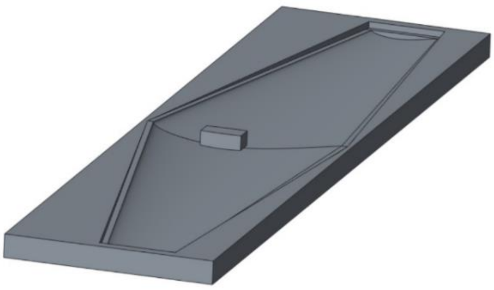

Figure E.1 The mold for the upper surface of the centerboard foil.

E.2 Building the molds

The molds were hollowed using a CNC milling machine. To prepare the necessary CAM operations, the finished CAD models of the molds were imported to the program *Fusion 360*. Here, all the operations and tool usages during the milling procedure were defined.

The molds were made from poplar. This is a soft type of wood, which means that it is easy to work with during milling and grinding [E1]. The CNC milling took place in the A-building’s wood workshop at LTH, see Figure E.2.

Figure E.2 CNC milling one of the molds.

After the milling was completed, some filler was added and grinding was applied in order to obtain the desired, smooth, surface finish. Finally, wax was applied to the molds to make sure that the carbon fiber foils could be easily removed from the molds at a later stage. One of the finished mold-halves of the centerboard strut can be seen in Figure E.3

Figure E.3 The right centerboard strut mold-half.

E.3 Arrangement of carbon fiber

The next step was to arrange the carbon fiber in the molds. Since the loads that would arise during hydrofoiling would vary in both strength and direction across the foils, different numbers of layers of carbon fiber were applied in different directions across the foil. Since the exact forces that would act on the foils during the dynamic load case were unknown, the arrangement was based on the experience of Oscar Wiberg, mechanical engineer at Corebon AB [E2]. The philosophy however was to be on the safe side and dimension the foils for far larger forces than they were ever expected to experience.

Two different weaves of carbon fiber were used. One unidirectional weave, where all fibers were oriented in the same direction, weighing 200 grams per square meter, and one multidirectional weave with fiber directions in $\pm 45^o$, weighing 400 grams per square meter. The arrangement of the carbon fiber for the centerboard struts are shown in Figure E.4 as an example.

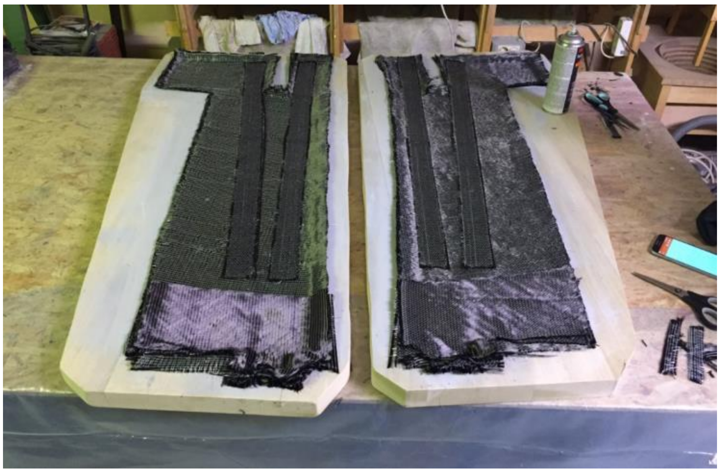

Figure E.4 Arrangement of carbon fiber.

E.4 The vacuum infusion process

The vacuum infusion process was used to inject epoxy into the mold where the carbon fiber was laid out. This process is schematically shown in Figure E.5, and is further described below [E3].

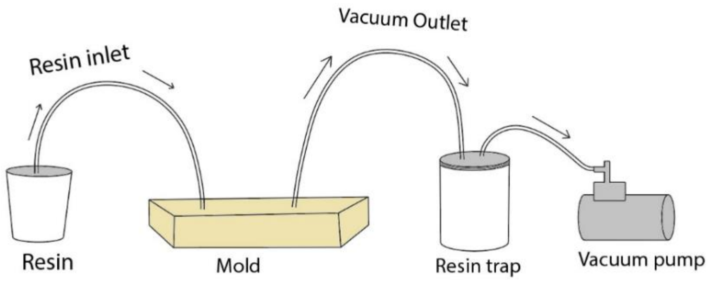

Figure E.5 The vacuum infusion process.

When the carbon fibers were arranged in the molds, the fibers were covered with a release film, a so-called peel ply, which can be seen in Figure E.6. This peel ply was easy to remove and would make sure that no other material would stick to the carbon fiber. The peel ply was also equipped with a large amount of small holes to make sure that the epoxy could reach the fibers from above.

Figure E.6 The carbon fiber covered with the peel ply.

On top of the release film, a distribution web was used to evenly distribute the epoxy over the entire surface of the mold, see Figure E.7.

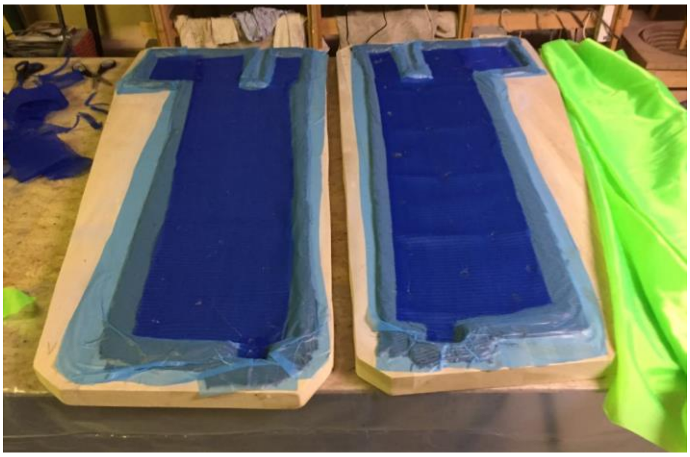

Figure E.7 The distribution web.

On this web, two tubes were glued: One tube to suck out the air, and one tube to inject the epoxy.

Finally, the entire mold was covered with a vacuum bag, which can be seen in Figure E.8. This vacuum bag was made out of simple construction foil and sealed with a special sealing tape.

Figure E.8 The molds covered with the vacuum bag.

The green material visible in the pictures above is a special kind of fabric that allows air to travel. The tube from the vacuum pump was connected directly to this fabric, which covered the edges of the carbon fiber. This meant that the air was sucked out of the entire area of the fabric instead from just one single point. This encouraged the epoxy to be spread out more efficiently over the fibers.

When the bag was sealed, it was connected to a vacuum pump. With the astounding force of this incredible piece of machinery, the air was sucked out of the bag, and a vacuum was created. The pump was left running for up to an hour to make sure that all of the air in the material of the molds would be removed. Meanwhile the bag was checked for any leaks. When the level of vacuum was satisfactory and no leaks had been found, the other tube was released into a bucket of epoxy. Thanks to the vacuum in the bag, the epoxy was sucked up through this tube and into the mold. Here, the distribution web made sure that the epoxy was distributed evenly among the fibers. Figure E.9 shows how the epoxy (the darker areas) is spread among the fibers.

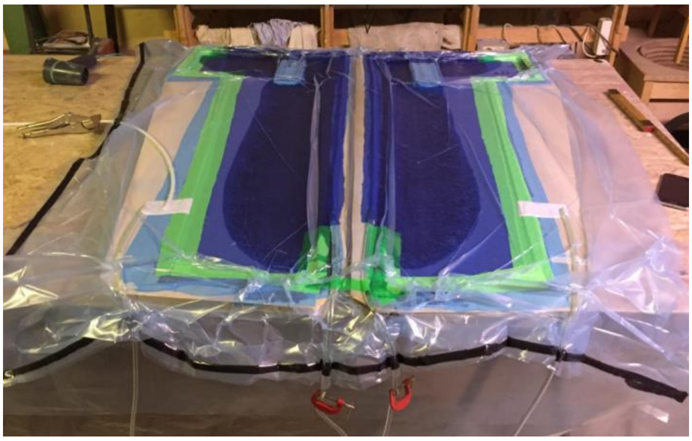

Figure E.9 Epoxy spreading among the fibers.

When the epoxy was injected to the fibers, it was left to harden. A heating fan was used to speed up the process. After about 12 hours, the epoxy had hardened and the foils could be removed from the molds.

E.5 Constructing the hinge

The hinge was made from fiberglass. It was important to make sure that the hinge was flexible enough. Therefore, some test pieces were created to study the effect the amount of layers, the fiber direction, and the width of the hinge had on the flexibility. These are shown in Figure E.10, numbered in chronological ascending order starting at 1 from the left.

Figure E.10 Fiberglass hinge test pieces.

The flexibility of one of the hinges can be seen being tested in Figure E.11.

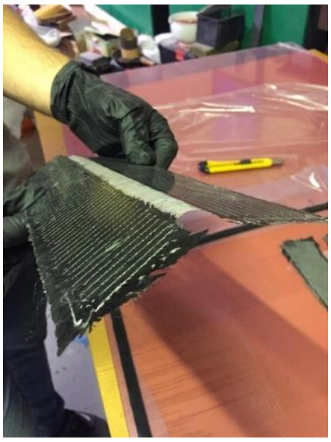

Figure E.11 Testing one of the hinges.

Data for the test pieces are shown in Table E.1.

Table E.1 Data for the different hinges tested.

Number	*Hinge width [mm]*	*Fiberglass direction*	*Number of layers*
1	15	90 degrees	1
2	20	90 degrees	1
3	25	90 degrees	1
4	15	45 degrees	1
5	20	45 degrees	2

As would be expected, the test pieces showed that a narrow hinge width meant a stiffer hinge. However, it also turned out that the hinge became more flexible with the fibers in the 45-degree direction compared to the 90-degree counterpart. This meant that the narrowest 45-degree hinge at 15 mm turned out to be more than flexible enough. The hinge made out of two layers was significantly stiffer, and would not work as an arrangement for the hinge.

Since hinge number 4 was more than flexible enough, it was decided to use the 45-degree orientation, but decrease the hinge width even further, to just 10 mm, for the real hinge.

Figure E.12 shows how the centerboard foil was constructed with the hinge. The upper surface (red), and the hinge (yellow) was built together as one single piece. The bottom surface was built as two separate parts (black and green).

Figure E.12 Illustration of how the centerboard foil was constructed.

The hinge was made directly in the mold of the upper surface of the centerboard foil. The first layers of carbon fiber were placed in the mold, then a slot of 10 mm were cut through these fibers, see Figure E.13.

On top of this slot, the fiberglass was placed, see Figure E.14. Thereafter, additional layers of carbon fiber were added (except for the area of the slot). When this special arrangement was done, it was covered with peel ply and distribution web, and finally injected with epoxy like all the other wings.

Figure E.13 The first layer of carbon fiber.

Figure E.14 The layer of fiberglass.

E.6 Post-processing the wing halves

When the wing halves were removed from the molds, the molding flash had to be cut and grinded away so that the wings got their intended shape. The rudder foil is shown directly out of its mold with the resulting flashes in Figure E.15, and after post-processing by cutting and grinding in Figure E.16.

Figure E.15 The rudder foil with molding flashes.

Figure E.16 The rudder foil with its intended shape.

Thereafter, the halves of the foils were provided with beams of ash to further strengthen the construction by improving its ability to transfer the shear forces between the two halves. This is shown in Figure E.17.

Figure E.17 The centerboard struts fitted with beams.

To be able to glue the two halves together later, a brink was made along the leading edge of each wing were the glue could be applied. This brink was made using an epoxy filler. The trailing edges were already flat enough for the glue to be applied directly without a brink. Also, the areas that would be affected by the connections of the struts and foil were filled with epoxy filler to increase the strength of these critical areas. This can be seen in Figure E.18.

Figure E.18 The centerboard strut with a brink along the leading edge.

At this stage, three M8 threaded rods were casted into the centerboard struts (intended for the future attachment of the centerboard in the centerboard gasket) which are visible in Figure E.19.

In the case of the centerboard strut, one of the halves were also fitted with a carbon fiber pipe near the trailing edge. In this pipe, the pushrod would move up and down to regulate the angle of the flap.

It was not desirable having the foils fill up with water when used, since this would increase the weight and thereby decrease the performance of the boat. It seemed unlikely that the foils would be able to be built perfectly waterproof. Thus, the solution was to fill the remaining volume with construction foam.

Figure E.19 The centerboard struts before they were glued together.

E.7 Gluing the wing halves together

The halves of the foils were now glued together using the composite glue *Crestabond* [E4]. This glue was applied along the leading edge, trailing edge, and along the beams. During this process, the lower halves of the wings were put back into their molds, to make sure that they did not become twisted or bent as they were joined together with their upper counterparts. The upper halves were put on top of the lower halves; to keep pressure on the joining foils, heavy sand bags were utilized. In Figure E.20, the centerboard strut can be seen with the two halves glued together.

Figure E.20 The two centerboard struts glued together.

E.8 Creating the centerboard plateau

When the centerboard strut was glued together, it was inserted into the centerboard case, while the boat was placed upside down. Thereafter, carbon fiber was put directly on the hull to get a perfect fit of to the boat. Release tape was used on the hull to prevent the carbon fiber from sticking to it. This process is shown in Figure E.21.

Figure E.21 Creating the plateau around the centerboard strut.

E.9 Connecting the struts to the foils

The glue used when joining the halves of the wings, was also used when connecting the foils to their struts. At this stage, it was important to be very accurate to make sure that the correct angles between the struts and foils were obtained. An inclined foil would have a negative effect on the performance.

E.10 Building the control system

The control system consisted of several parts which are described below.

Due to its complex geometry, the *plate* was manufactured through 3D printing. The part was however too large to be 3D printed at the facilities at Lund University. Instead, Essiq AB contacted the company *GT Prototyper*, whom were friendly enough to 3D print this part for free.

The *lever* also had a complex geometry, and was therefore 3D printed as well. This smaller part was printed at the facilities of Lund University.

The *wand* was simply made out of a carbon pipe cut to the right length. The wand was thereafter fitted with a plate at one end to create enough resistance for the wand to follow the surface of the water.

The *pushrod* was made out of a single pipe of stainless steel with a diameter of 3 mm, and cut to the right length.

The *seesaw* was made by a turnbuckle welded to a small Ø8 mm stainless steel rod.

The *vertical link* was made by cutting a piece of aluminum and drilling a series of holes.

E.11 Fitting the hydrofoils to the hull

The intention was to fit the hydrofoils to the hull without making any permanent changes to it. Below it is explained how this was done.

As described in section E.8, the centerboard was fitted with a plateau directly underneath the hull. This plateau holds the entire weight of the boat. Due to the plateau, the centerboard had to be inserted from underneath the hull. The three threaded rods that were casted into the top side of the strut were long enough to pass through the upper surface of the centerboard case. On top of the centerboard case, the *plate* was placed. The *plate* was used for the control system, but also had the function of a large “washer”. The threaded rods from the centerboard passed through three holes in this *plate* and were fixed with wingnuts. The installed *plate* can be seen in Figure E.22 below.

Figure E.22 The plate fitted to the centerboard case.

The hull of the Europe-dinghy is normally fitted with two strips around the centerboard slot to prevent water from splashing up through it.

The part of the strut that should fit inside the centerboard case needs to have a tight fit to be able to transfer the forces from the centerboard to the case in the most efficient way possible. This, combined with the fact that the centerboard had to be inserted from underneath, made it impossible to keep the centerboard slot stripes. This is not a problem when using the hydrofoils, since the plateau effectively covers the slot. However, if the sailor one day would like to use the dinghy using the normal centerboard and rudder, the absence of these strips would be a problem. It is not very practical having to reattach and remove them every time the sailor decides to switch between foiling and regular sailing. Unfortunately, during this project, no solution to this problem was found.

Since the ambition was to avoid making changes to the hull, the existing rudder fittings on the hull were used during the test run. If it had turned out that these were not strong enough to withstand the increased forces during foiling, new stronger ones would easily have been attached.

To save time, the standard Europe-dinghy rudder head was used, instead of building a new one. The original rudder head was constructed so that when foiling, the weight of the hull was supported by only one of the rudder fittings. Therefore, the rudder head was modified, so that the weight would be evenly distributed between the two fittings on the hull. The modifications of the rudder head can be seen in Figure E.23 (The wooden part that the uppermost rudder fitting is resting on).

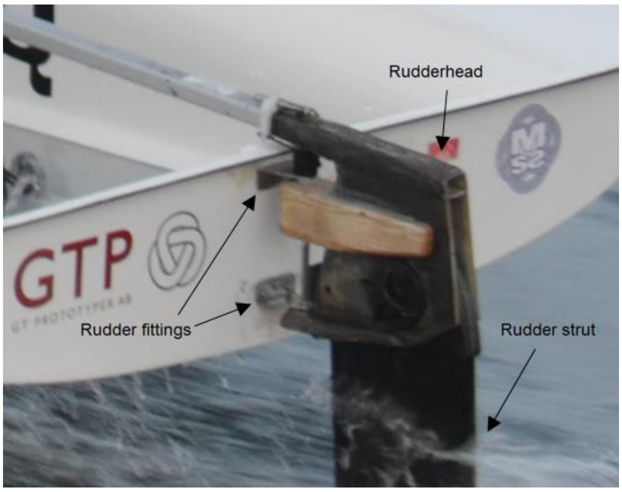

Figure E.23 The rudder head fitted to the boat.

The angle of the rudder on a regular Europe-dinghy is fixed through friction by clamping the rudder in the rudder head, as can be seen in Figure E.23. It was decided to try the same system for fixing the angle of the new rudder equipped with foils.

References Appendix E

[E1] The wood database, Poplar. (n.d.). Retrieved January 2, 2018, from http://www.wood-database.com/poplar/

[E2] Wiberg, O., Mechanical Engineer, Corebon AB, Malmö, Sweden. Personal conversations (2017).

[E3] Vacuum Infusion Process. (n.d.). Retrieved January 3, 2018, from http://www.performancecomposites.com/about-composites-technical-info/125-resin-vacuum-infusion.html

[E4] Crestabond® M1-20. (2018). Retrieved January 3, 2018, from http://www.scottbader.com/adhesives/selector/328/crestabond-m1-20

Appendix F Drawings

In this Appendix, simplified drawings of the finished prototype are presented.

Simplified assembly drawings are presented in Figure F.1-F.4. Thereafter, simplified drawings of each component are shown in Figure F.5-F.8.

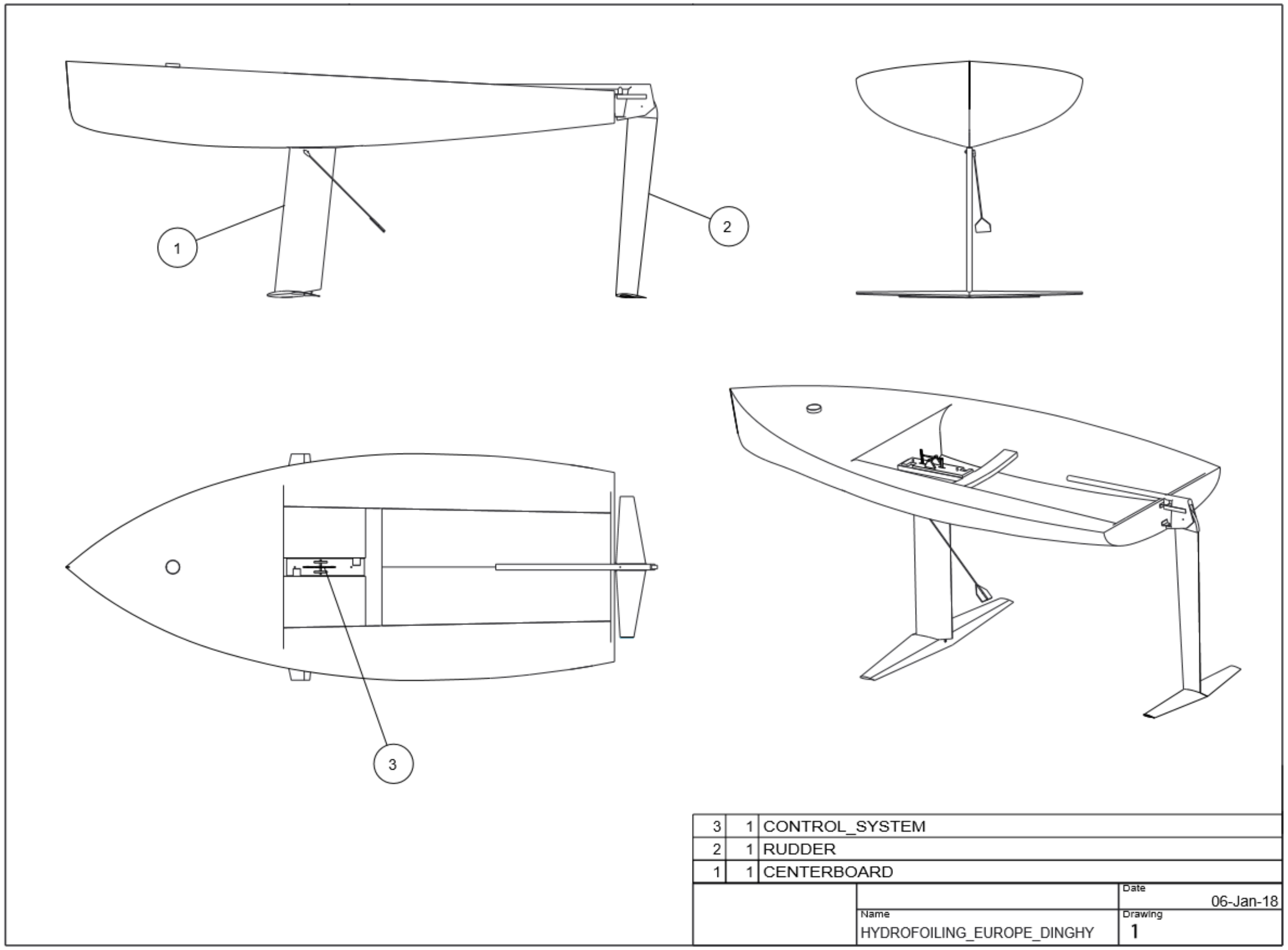

Figure F.1 Simplified drawing over the assembled dinghy.

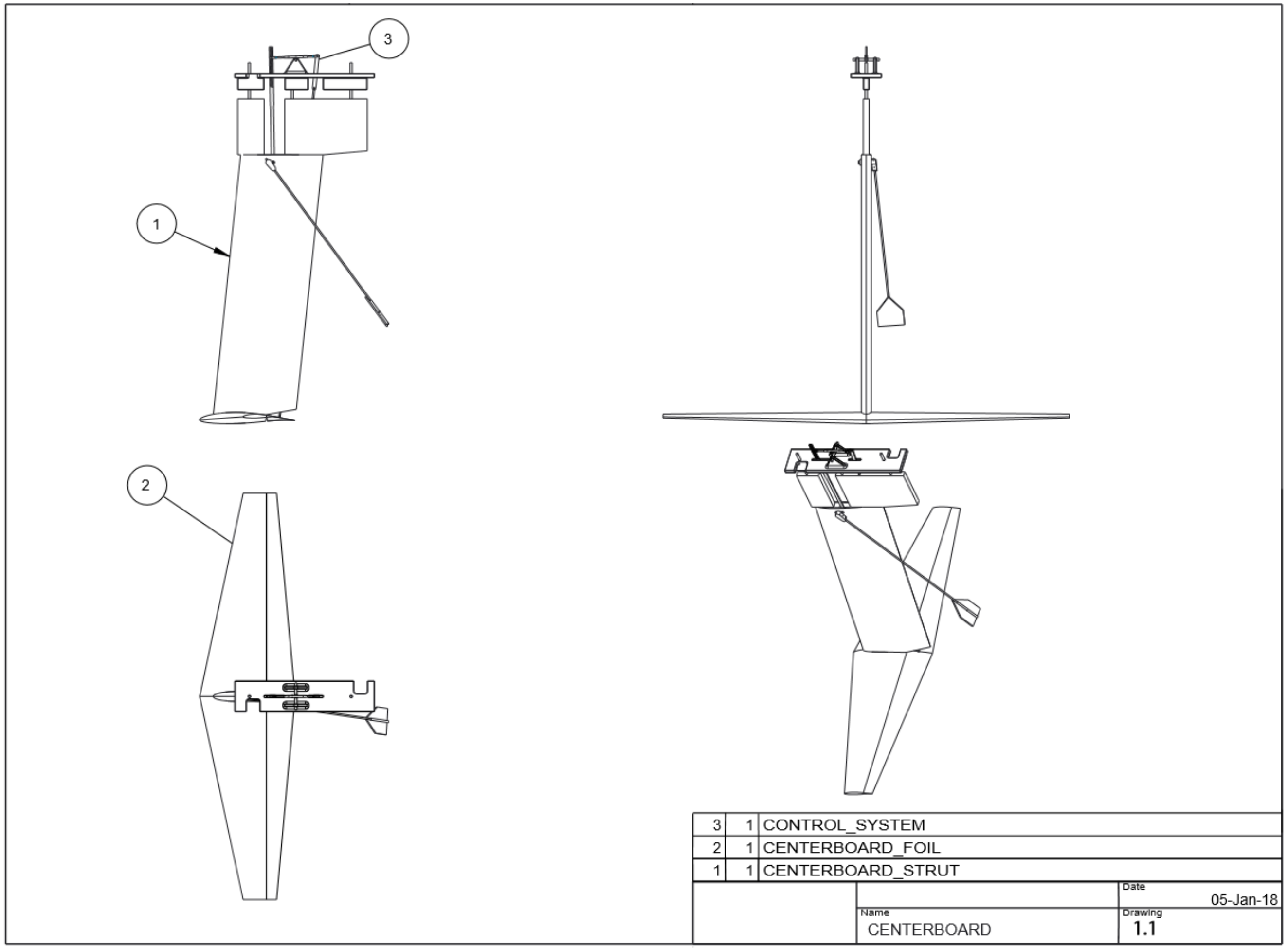

Figure F.2 Simplified drawing of the centerboard assembly.

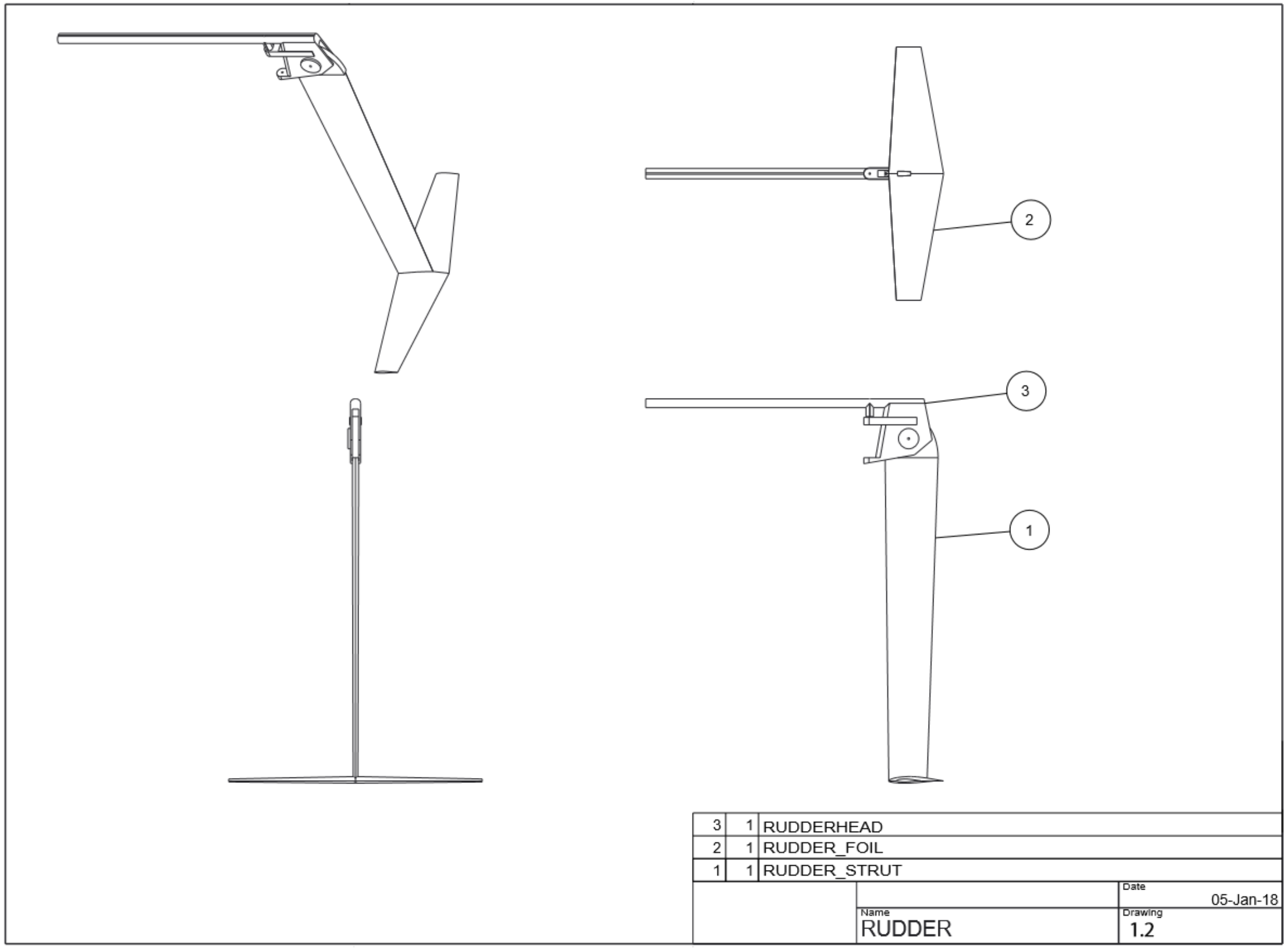

Figure F.3 Simplified drawing of the rudder assembly.

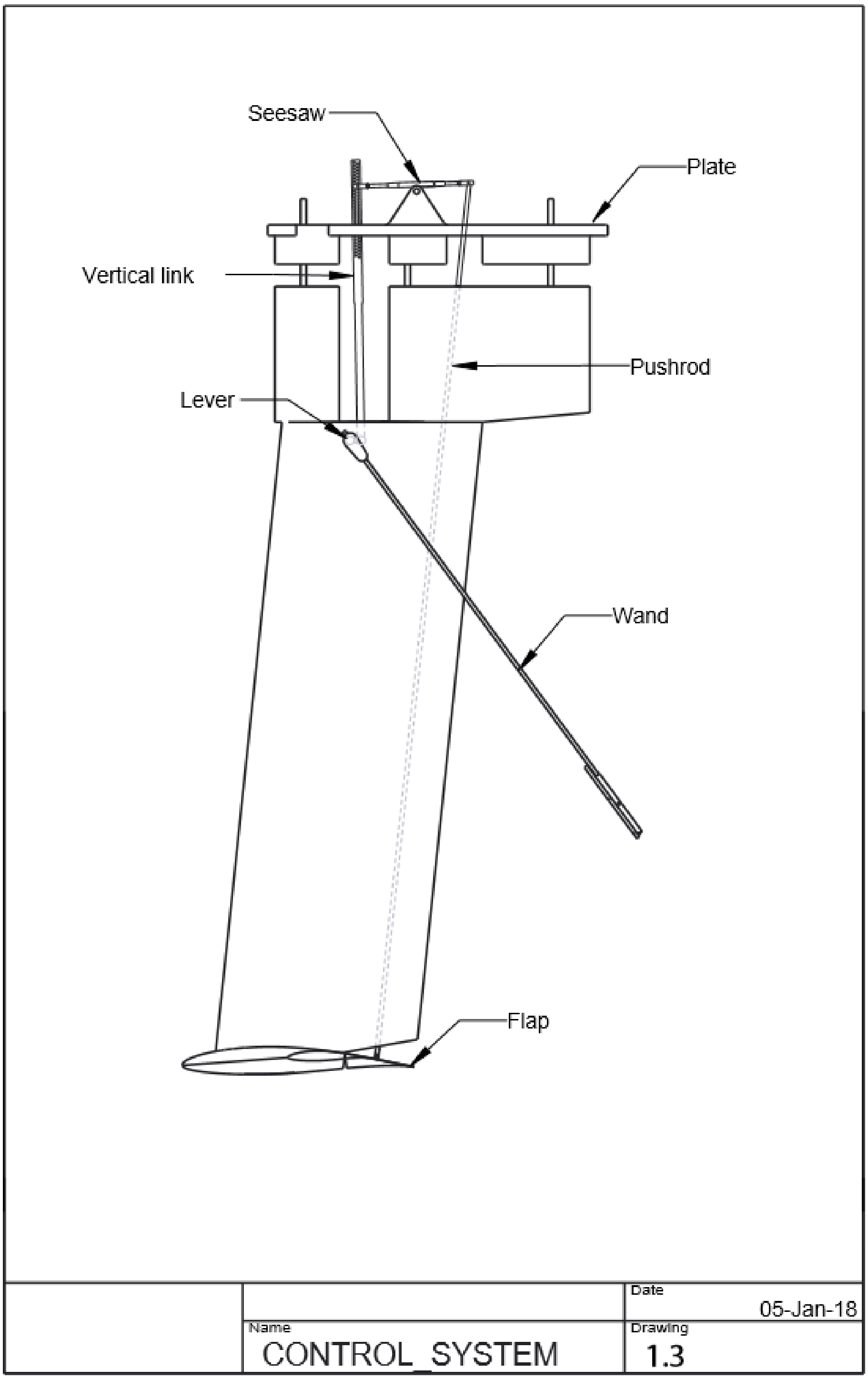

Figure F.4 Simplified drawing of the control system assembly.

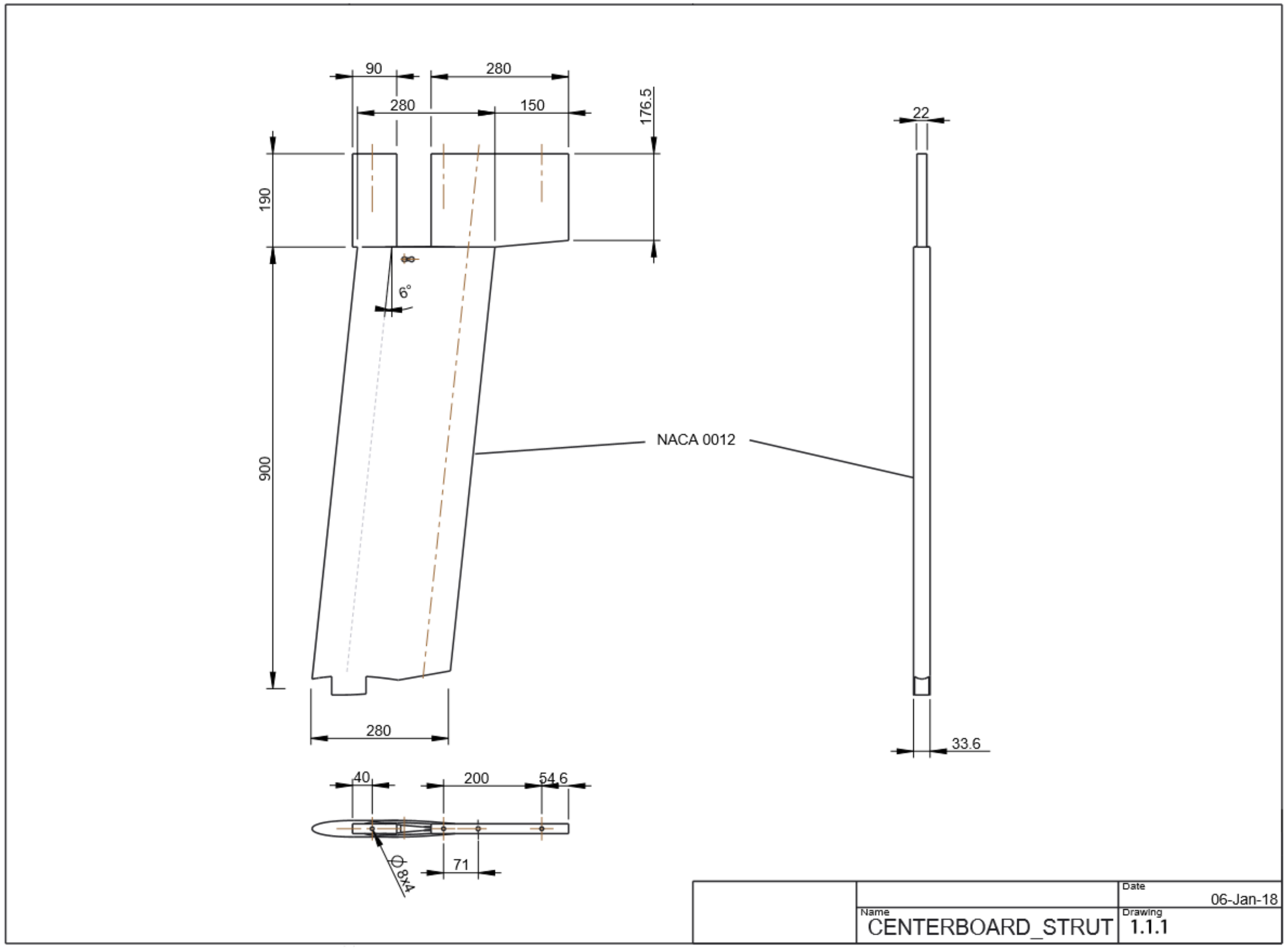

Figure F.5 Simplified drawing of the centerboard strut.

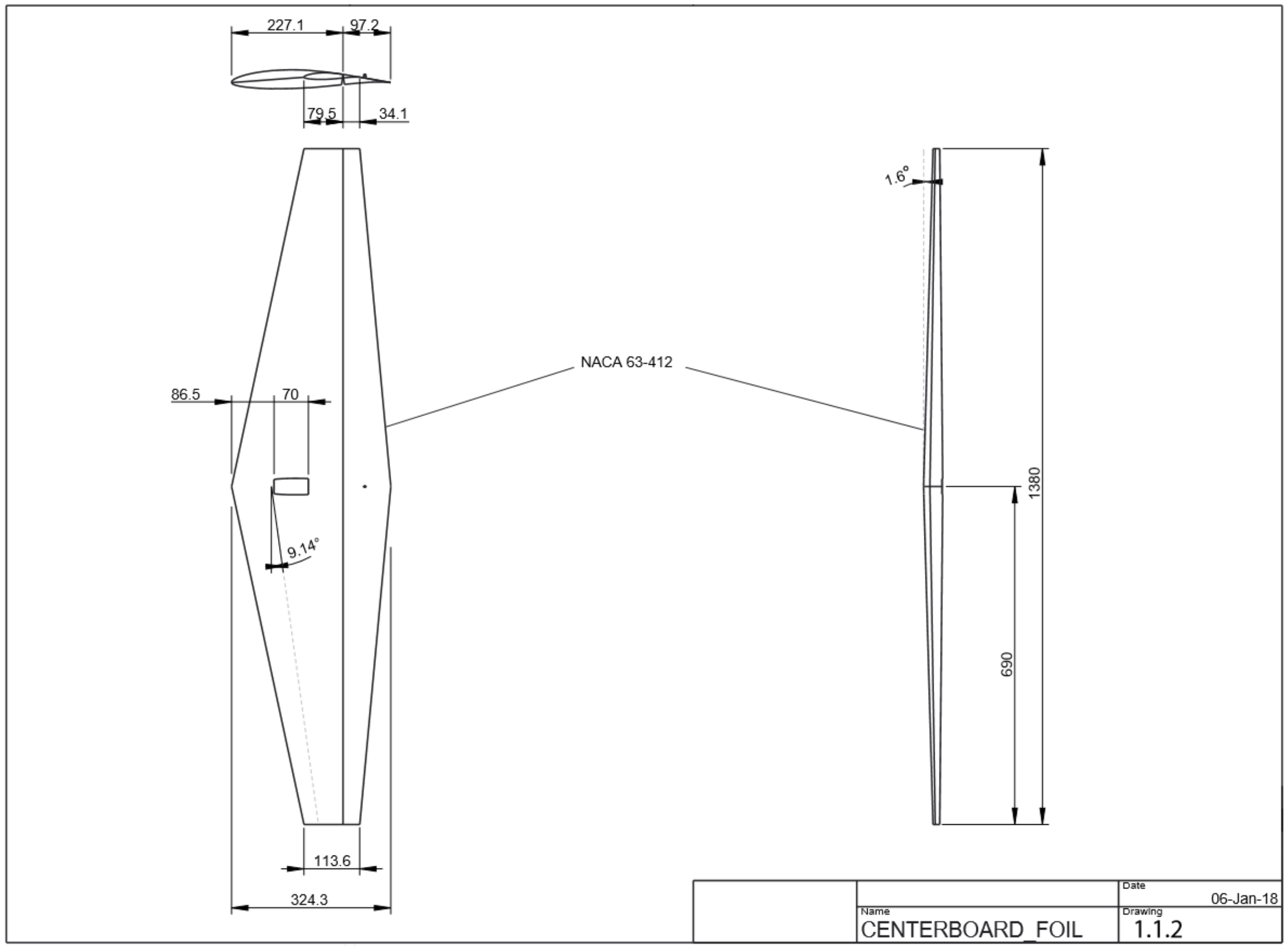

Figure F.6 Simplified drawing of the centerboard foil.

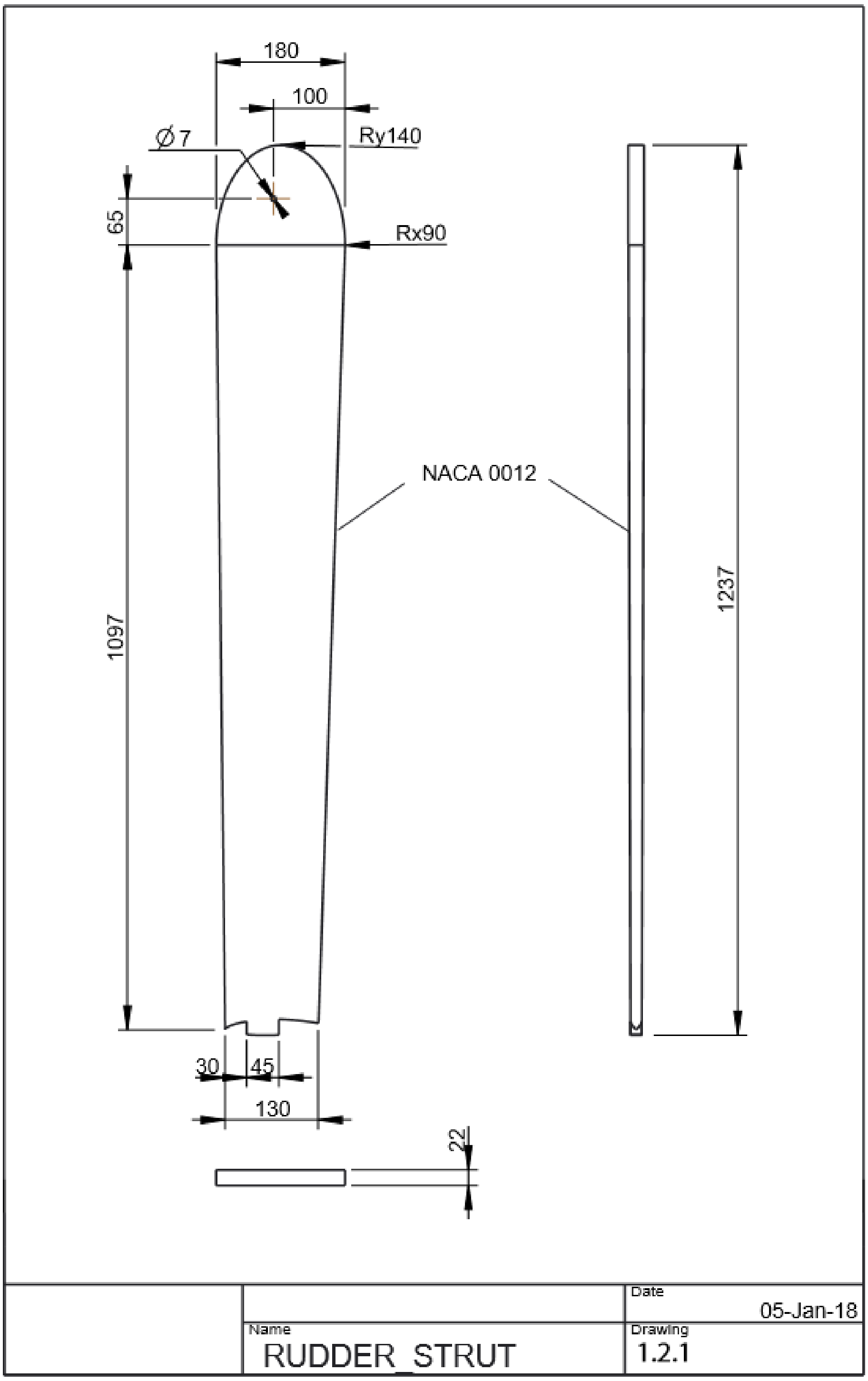

Figure F.7 Simplified drawing of the rudder strut.

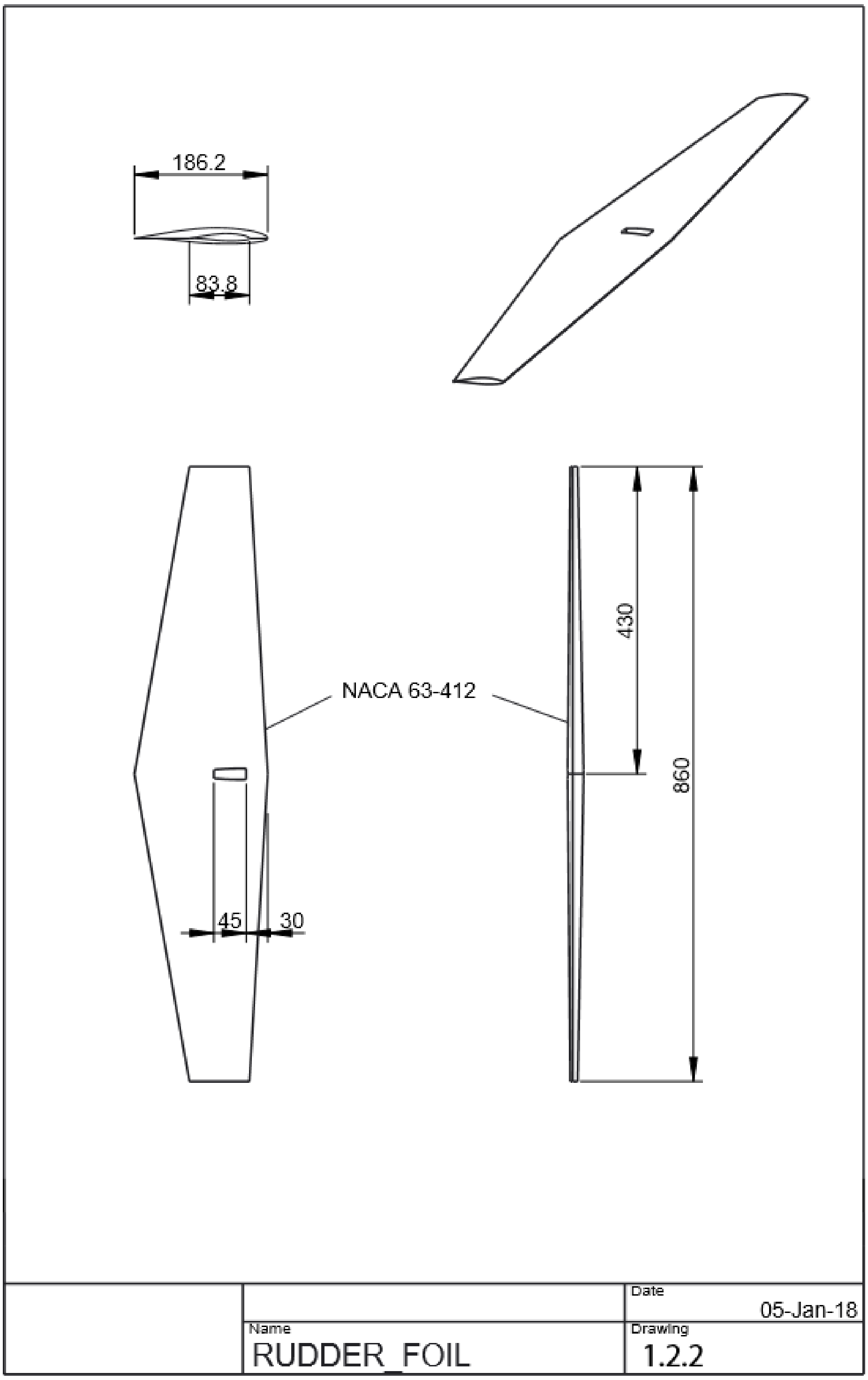

Figure F.8 Simplified drawing of the rudder foil.

Appendix G Time plan and work distribution

In this Appendix, the time plan and the work distribution is presented.

G.1 Time plan

The timeline for the project can be seen below in Table G.1. The table contains both the planned timeline, and the timeline as the project actually turned out – the effective timeline. As can be seen, the work went according to plan for the first couple of weeks, and the build of the prototype started on schedule. However, since both the authors lacked experience in building projects of this nature, the time necessary to build was underestimated. This also resulted in less time to test the prototype. The sharp-eyed reader might notice one other major difference between the planned timeline and the effective one, namely writing the report. The explanation for this is extensive and complicated, and will therefore not be discussed any further here.

Table G.1 The planned and effective timeline

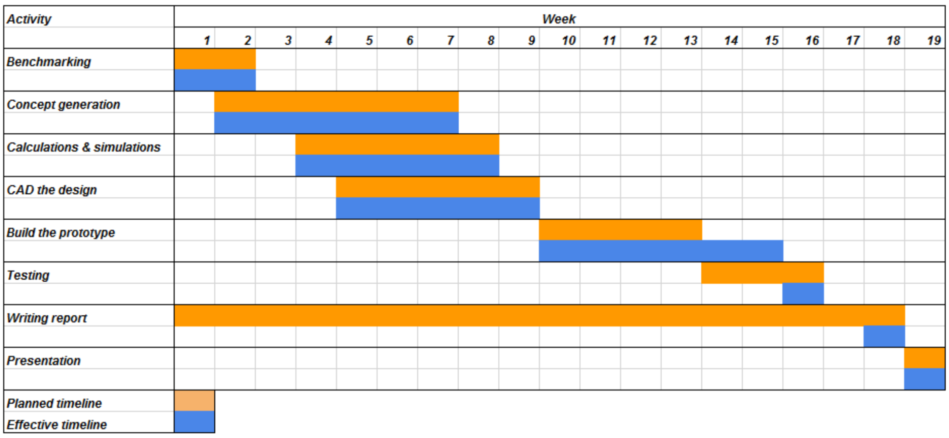

G.2 Work distribution

The majority of the different activates during this project has been performed in a collaboration between both authors. At a few points however, they have been working separately on different things to make the work process more effective. At the early stages of the project, Jesper was responsible for the calculations made in XFOIL, while Simon derived the different expressions needed to calculate takeoff speed, etc. The different concepts were developed together, to incorporate as many different points of views as possible. Both authors were involved with the 3D modelling of the final design, working in close proximity to make sure that all the various parts would work together. When the design was finished, Jesper was responsible for creating the CAD models of the molds, while Simon were preparing for the build by contacting different suppliers to make sure that all material and components needed for the build was in place. The building phase was carried out in collaboration by both authors.